Supporting Information

Nuclear Localization Signals Enable the Cellular Delivery of an Anti-CRISPR Protein to Control Genome Editing

Axel O. Vera,[†,‡] Franklin J. Avilés-Vázquez,[§,∥] Taekjip Ha,[§,⊥] Amit Choudhary,[*,‡,#,▽] and Ronald T. Raines[*,†,○]

[†]Department of Chemistry, Massachusetts Institute of Technology, Cambridge, Massachusetts 02139, United States
[‡]Chemical Biology and Therapeutics Science Program, Broad Institute of MIT and Harvard, Cambridge, Massachusetts 02142, United States
[§]Howard Hughes Medical Institute and Program in Cellular and Molecular Medicine, Boston Children's Hospital, Boston, Massachusetts 02115, United States
[∥]Department of Biophysics and Biophysical Chemistry, Johns Hopkins University, Baltimore, Maryland 21218, United States
[⊥]Department of Pediatrics, Harvard Medical School, Boston, Massachusetts 02115, United States
[#]Divisions of Renal Medicine and Engineering, Brigham and Women's Hospital, Boston, Massachusetts 02115, United States
[▽]Department of Medicine, Harvard Medical School, Boston, Massachusetts 02115, United States
[○]Koch Institute for Integrative Cancer Research at MIT, Massachusetts Institute of Technology, Cambridge, Massachusetts 02139, United States

*E-mail: achoudhary@bwh.harvard.edu; rtraines@mit.edu

Downloaded from pubs.acs.org/jacsat/article-supplement/5420577/pdf/ja5c19089_si_001/ by guest on 21 November 2026

Table of Contents

Materials and Methods

Conditions S4
Recombinant DNA S4
Protein Purification S4
Cell Culture S4
Acr Addition/Delivery to Cells S5
GFP-Disruption Assay S5
GFP-Disruption Assay (3D Cell Cultures) S6
HiBiT Knock-In Assay (HUES 8 Cells) S6
HiBiT Knock-In Assay (HEK293T Cells) S6
Next-Generation Sequencing S7
Direct Visualization of Anti-CRISPR–Mediated Cas9–GFP Inhibition S7
Fluorescently Labeling Anti-CRISPR Proteins S7
Direct Visualization of Anti-CRISPR Delivery S8

Supplementary Tables

Table S1 ..... S9
Table S2 ..... S9
Table S3 ..... S10
Table S4 ..... S11
Table S5 ..... S11
Table S6 ..... S12
Table S7 ..... S12
Table S8 ..... S12
Table S9 ..... S12
Table S10 ..... S13
Table S11 ..... S14
Table S12 ..... S14

Supplementary Figures

Figure S1 ..... S15
Figure S2 ..... S16
Figure S3 ..... S17
Figure S4 ..... S18
Figure S5 ..... S19
Figure S6 ..... S20
Figure S7 ..... S21
Figure S8 ..... S22
Figure S9 ..... S23
Figure S10 ..... S24
Figure S11 ..... S25
Figure S12 ..... S26

Downloaded from pubs.acs.org/jacsat/article-supplement/5420577/pdf/ja5c19089_si_001/ by guest on 21 November 2026

Figure S13 ..... S27
Figure S14 ..... S28
Figure S15 ..... S29
Figure S16 ..... S30
Figure S17 ..... S31
Figure S18 ..... S32
Figure S19 ..... S33
Figure S20 ..... S34
Figure S21 ..... S35
Figure S22 ..... S36
Figure S23 ..... S37
Figure S24 ..... S38
Figure S25 ..... S39
Figure S26 ..... S45
Figure S27 ..... S46
Figure S28 ..... S47
Figure S29 ..... S48
Figure S30 ..... S49
Figure S31 ..... S50
Figure S32 ..... S52
Figure S33 ..... S53
Figure S34 ..... S54
Figure S35 ..... S55
Figure S36 ..... S59
Figure S37 ..... S60
Figure S38 ..... S61
Figure S39 ..... S62
Figure S40 ..... S63

Plasmid Sequence

pAV13-MBP-TEV-4×NLS-Cys-AcrIIA4-2×NLS S67

Equations S70

References S71

Downloaded from pubs.acs.org/jacsat/article-supplement/5420577/pdf/ja5c19089_si_001/ by guest on 21 November 2026

Materials and Methods

Conditions

All procedures were performed in air at ambient temperature (~22 °C) and pressure (1.0 atm) unless indicated otherwise.

Recombinant DNA

A DNA fragment encoding the sequence of Cys-AcrIIA4 was inserted downstream of a 6×His tag, maltose binding protein (MBP), a TEV protease cleavage site, and a 4×SV40 NLS tag and upstream of a C-terminal 2×SV40 NLS tag in a custom vector (Addgene plasmid #88917)[1] by Gibson assembly to generate a plasmid for bacterial production and purification of 6×NLS-Acr (pAV13-MBP-TEV-4×NLS-Cys-AcrIIA4-2×NLS).

Protein Purification

pAV14, pAV17, and pAV18 plasmids were used to produce and purify LF_N-Acr, 0×NLS-Acr and 1×NLS-Acr, as previously described.[2] 6×NLS-Acr was purified using the following method: *Escherichia coli* Rosetta2 (DE3) cells transformed with pAV13 were cultured in Lysogeny Broth supplemented with 100 μg/mL ampicillin and 2% w/v glucose at 37 °C for 16 h. The starter culture was subcultured in Terrific Broth supplemented with 100 μg/mL ampicillin and 2% w/v glucose at 37 °C until the OD_{600} was 0.6–0.8. Protein production was induced with 500 μM isopropyl-β-D-thiogalactoside (IPTG), and the cultures were grown at 16 °C for 16 h. The cells were harvested, resuspended in lysis buffer (20 mM Tris–HCl buffer, pH 7.5, containing 500 mM NaCl, 20 mM imidazole, 1 mM tris(2-carboxyethyl)phosphine (TCEP), and 5% v/v glycerol) supplemented with 0.5 mM phenylmethanesulfonyl fluoride and Roche cOmplete Protease Inhibitor Cocktail, and lysed by sonication. MBP–6×NLS-Acr was purified using Ni-NTA Superflow resin (Qiagen, 30410) in lysis buffer supplemented with either 20 mM imidazole (wash) or 300 mM imidazole (elution). Eluted MBP–6×NLS-Acr was cleaved with TEV protease (purified in-house using Addgene plasmid #8827)[3] overnight at 4 °C and dialyzed into 20 mM HEPES buffer, pH 7.5, containing 300 mM NaCl, 1 mM TCEP, and 5% v/v glycerol. Cleaved 6×NLS-Acr was loaded onto an MBPTrap HP (Cytiva, 28918779) upstream of a HiTrap SP HP (Cytiva, 17115201). 6×NLS-Acr was eluted over a linear gradient of NaCl (0.3–1.00 M) in 20 mM HEPES–HCl buffer, pH 7.5, containing 1 mM TCEP and 5% v/v glycerol. 6×NLS-Acr was then loaded onto a HiLoad 16/600 Superdex 200 pg (Cytiva, 28989335) and eluted with 20 mM HEPES–HCl buffer, pH 7.5, containing 500 mM NaCl, 1 mM TCEP, and 5% v/v glycerol. Acr concentration was measured using $A_{280\ nm}$ or using the BCA and Bradford assays (Thermo Fisher Scientific). Acr purity was assessed by SDS–PAGE (Coomassie blue staining) and Q-TOF LC–MS.

Cell Culture

U2OS cells, U2OS cells with an integrated *GFP–PEST* fusion gene (U2OS-EFFP.PEST), U2OS cells stably expressing Cas9–GFP and 53BP1–mCherry (U2OS-Cas9-GFP), and HEK293T cells were cultured in Dulbecco's modified Eagle's medium with GlutaMax (DMEM, Gibco, 10564-011) supplemented with 10% v/v fetal bovine serum (FBS, Corning, 35-016-CV), 100 U/mL penicillin−streptomycin (Gibco, 15140-122), and 1 mM sodium pyruvate (Gibco, 11360-070) at

Downloaded from pubs.acs.org/jacsat/article-supplement/5420577/pdf/ja5c19089_si_001/ by guest on 21 November 2026

37 °C in a 5% v/v CO_2(g) atmosphere. INS-1E rat β-cells were cultured in Roswell Park Memorial Institute (RPMI) medium (Gibco, 11875-093) supplemented with 10% FBS, 1 mM pyruvate, 100 U/mL penicillin-streptomycin, and 50 μM of 2-mercaptoethanol. FBS was never removed from the medium for Acr delivery experiments in U2OS cell lines, INS-1E rat β-cells, and HEK293T cells. HUES 8 cells (Harvard Stem Cell Institute iPS Core Facility) were cultured in mTeSR1 medium (STEMCELL Technologies, 85850) over a Matrigel-coated surface (Corning, 356234) at 37 °C in a 5% v/v CO_2(g) atmosphere. mTeSR1 medium was supplemented with 10 μM ROCK inhibitor Y-27632 (Enzo Life Sciences, ALX-270-333) for cell splitting and genome editing experiments.

Acr Addition/Delivery to Cells

At a 0-h dosing time or time point, Cas9-transfected cells were treated with Acrs immediately before starting the incubation at 37 °C. At a >0-h dosing time or time point, Cas9-transfected cells were treated with Acrs >0 h after starting the incubation at 37 °C. Cas9 transfection refers to delivering Cas9 into cells either via nucleofection or lipofection. For dose-dependency studies at 2 h in the *GFP* disruption assay, Acrs (0.125–4 μM) were added to the cells 2 h after Cas9 transfection by replacing the cell culture medium in the well with fresh medium containing the Acrs diluted to the desired concentration. The final buffer concentration in the medium was <1% v/v at all times. For dose-dependency studies at 0 h or for time-dependency studies at a constant concentration, Acrs (0.125–4 μM) were added to the cells 0–24 h (excluding 2 h) after Cas9 transfection by directly pipetting an Acr stock solution in buffer to the cell culture medium in the well. The Acr stock solution was prepared so that, upon dilution, the final buffer concentration in the medium was 4.8% v/v (e.g., adding 5 μL of Acr stock solution to 100 μL of cell culture medium).

GFP-Disruption Assay

SpCas9-NLS RNP (20 pmol) targeting the *GFP* gene was delivered via nucleofection into U2OS-EGFP.PEST cells (300,000 cells) using an SE Cell Line 4D-Nucleofector X Kit (Lonza, V4SC-1096, DN-100 protocol). The nucleofected cells were resuspended in cell culture medium (100,000 cells/mL), transferred to a Revvity (6055302) 96-well PhenoPlate (100 μL), and incubated at 37 °C. 0–24 h after starting the incubation (dosing time), 0×NLS-Acr, 1×NLS-Acr, or 6×NLS-Acr were added to the cells via the medium-exchange (2-h dosing time) or direct addition method (all other dosing times). After 48 h, live cells were stained with 2 μg/mL Hoechst 33342 (37 °C, 20 min) in FluoroBrite DMEM (Gibco, A1896701) and imaged using high-throughput confocal microscopy on a Revvity Opera Phenix microscope equipped with a 20× objective, which enabled detection of GFP (green) and Hoechst 33342 (blue) fluorescence upon 488 nm and 405 nm laser excitation. Digital phase contrast (DPC) images were acquired using the same microscope. Images were analyzed using Revvity Harmony Software. Cells were selected based on the Hoechst 33343 nuclear stain, and the cell region was defined using digital phase contrast. A mean GFP threshold intensity was chosen by comparing ApoCas9- and Cas9 RNP-nucleofected cells. The distribution of cells above this threshold (GFP positive) was used to determine % *GFP* disruption. Cas9-mediated cleavage disrupts the *GFP* gene. Acr delivery prevents Cas9-mediated *GFP* disruption.

Downloaded from pubs.acs.org/jacsat/article-supplement/5420577/pdf/ja5c19089_si_001/ by guest on 21 November 2026

GFP-Disruption Assay (3D Cell Cultures)

SpCas9-NLS RNP (20 pmol) targeting the *GFP* gene was delivered via nucleofection into U2OS-EGFP.PEST cells (300,000 cells) using an SE Cell Line 4D-Nucleofector X Kit (Lonza, V4SC-1096, DN-100 protocol). The nucleofected cells were resuspended in cell culture medium (850,000 cells/mL), transferred to a Revvity (6055330) CellCarrier Spheroid ULA 96-well plate (100 μL), and incubated at 37 °C. 7–13 h after starting the incubation (dosing time), 6×NLS-Acr (2.5 μM) was added to the cells by the direct addition of a concentrated 6×NLS-Acr solution (5 μL). After 48 h, live cells were imaged using high-throughput confocal microscopy on a Revvity Opera Phenix microscope equipped with a 5× objective, which enabled detection of GFP (green) fluorescence upon 488 nm laser excitation. Brightfield images were acquired using the same microscope. Live-cell imaging was also performed before the addition of 6×NLS-Acr at 7 and 13 h. The 48-h images were analyzed using Revvity Harmony Software. The spheroid region was defined based on residual GFP fluorescence and partitioned into an outer, entire, and inner spheroid region (Figure S16). The mean GFP intensity in each region was used to determine % *GFP* disruption. Cas9-mediated cleavage disrupts the *GFP* gene. Successful delivery of 6×NLS-Acr prevents Cas9-mediated *GFP* disruption.

HiBiT Knock-In Assay (HUES 8 Cells)

SpCas9-NLS RNP (20 pmol) targeting the *GAPDH* gene and the HiBiT ssODN (80 pmol) were delivered via nucleofection into HUES 8 cells (450,000 cells) using a P3 Primary Cell 4D-Nucleofector X Kit (Lonza, V4XP-3032, CA-137 protocol). The nucleofected cells were resuspended in mTeSR1 medium supplemented with 10 μM Y-27632 (420,000 cells/mL), transferred to a Matrigel-coated 96-well plate (100 μL), and incubated at 37 °C. Cells were treated with 0×NLS-Acr or 6×NLS-Acr (0.125–4 μM) 0–16 h after starting the incubation (dosing time). After 24 h, the cells were incubated with the PrestoBlue HS reagent (Thermo Fisher Scientific, P50200), and their viability was measured using fluorescence spectroscopy (560 nm excitation/590 nm emission, SpectraMax M5). The cells were lysed in the presence of LgBiT and furimazine (Nano-Glo HiBiT Lytic Detection System, Promega, N3030), and their luminescence was quantified (Perkin Elmer EnVison). Cas9-mediated cleavage and HiBiT tag insertion via homology-directed repair produce NanoLuc after adding LgBiT and furimazine. Acr delivery prevents Cas9-mediated cleavage, HiBiT tag insertion, and NanoLuc formation.

HiBiT Knock-In Assay (HEK293T Cells)

SpCas9-NLS RNP (20 pmol) targeting the *GAPDH* gene and the HiBiT ssODN (80 pmol) were delivered via nucleofection into HEK293T cells (300,000 cells) using an SF Cell Line 4D-Nucleofector X Kit (Lonza, V4SC-2096, CM-130 protocol). The nucleofected cells were resuspended in cell culture medium (150,000 cells/mL), transferred to a poly(D-lysine)-coated 96-well plate (100 μL), and incubated at 37 °C. Cells were treated with 0×NLS-Acr or 6×NLS-Acr (0.4–1.5 μM) at 0 h. After 72 h, the cells were incubated with the PrestoBlue HS reagent (Thermo Fisher Scientific, P50200), and their viability was measured using fluorescence spectroscopy (560 nm excitation/590 nm emission, SpectraMax M5). The cells were lysed in the presence of LgBiT and furimazine (Nano-Glo HiBiT Lytic Detection System, Promega, N3030), and their luminescence was quantified (Perkin Elmer EnVison). Cas9-mediated cleavage and HiBiT tag

Downloaded from pubs.acs.org/jacsat/article-supplement/5420577/pdf/ja5c19089_si_001/ by guest on 21 November 2026

insertion via homology-directed repair produce NanoLuc after adding LgBiT and furimazine. Acr delivery prevents Cas9-mediated cleavage, HiBiT tag insertion, and NanoLuc formation.

Next-Generation Sequencing

HEK293T cells were seeded at 150,000 cells per well in 571.4 μL of cell culture medium on a poly(D-lysine)-coated 24-well plate and incubated at 37 °C. After 24 h, the cells were transfected via lipofection (Lipofectamine 3000, Invitrogen, L3000-015) with plasmids encoding 2×NLS-SpCas9 (750 ng, Addgene plasmid #42230)[4] and *EMX1*-targeting gRNA (250 ng).[5] Cells were treated with 0×NLS-Acr (4 μM), 6×NLS-Acr (4 μM), or LF_N-Acr (250 nM) ± PA (20 nM) at 1 h. After 72 h, genomic DNA was extracted (QIAamp DNA Mini Kit, Qiagen, 51304) and the target and off-target sites were PCR amplified, barcoded, and purified by gel extraction (MinElute Gel Extraction Kit, Qiagen, 28604). The amplicons were sequenced with NGS and analyzed using the CRISPResso2 software pipeline to determine % modification.

Direct Visualization of Anti-CRISPR–Mediated Cas9–GFP Inhibition

U2OS cells stably expressing Cas9–GFP and 53BP1–mCherry fusion proteins (U2OS-Cas9-GFP cells) were seeded at 100,000 cells per well in 100 μL of cell culture medium on a 10 mm microwell inside a 35 mm glass-bottom dish. The dish was then covered with 1.9 mL of cell culture medium and incubated at 37 °C. After 24 h, the cells were transfected via lipofection (RNAiMAX, Invitrogen, 13778-030) with a truncated gRNA that targets a highly repetitive region on chromosome 3 (Ch3 gRNA). Cells were treated with 0×NLS-Acr (2.5 μM), 6×NLS-Acr (2.5 μM), or LF_N-Acr (2.5 μM) ± PA (20 nM) either 0.5 h before (−0.5 h) or 15 h after (15 h) gRNA transfection. Before imaging, live cells were washed with Leibovitz's L-15 medium supplemented with 10% v/v FBS and 100 U/mL penicillin-streptomycin and maintained in this medium. Cells were imaged using widefield fluorescence microscopy at 15 and 20 h for −0.5- and 15-h Acr treatments, respectively. A Nikon Ti-E fluorescence microscope, equipped with a 60× objective and a stage-top incubator at 37 °C, was used to detect Cas9–GFP and 53BP1–mCherry fluorescence upon 485 nm and 560 nm laser excitation. Emission was collected using 525/50 nm and 630/75 nm filters, respectively. Z-stacks (25 slices, 0.5 μm step size) encompassing the entire nuclear volume were acquired using dual Hamamatsu C9100-13 EMCCD cameras. Image analysis was performed using a custom pipeline in a Python-based Jupyter notebook. In brief, nuclei were segmented from the 53BP1–mCherry channel using a voxel-aware watershed algorithm (skimage.segmentation.watershed) after generating seeds from the local maxima of a Gaussian-filtered image (sigma = 2 pixels). Cas9–GFP foci were identified in 3D by first applying a rolling-ball background subtraction (ball radius = 5 pixels) followed by white-tophat filtering (ball radius = 3 pixels) to enhance punctate features. Candidate foci were then localized using the DAOStarFinder class from Photutils with a detection threshold of 5 standard deviations above the local background and a full-width at half-maximum (FWHM) of 3 pixels. Finally, the integrated intensity of each focus was measured using an ellipsoidal aperture (semi-major axis = 3 pixels), with local background subtraction from a concentric ring (inner radius = 4 pixels, outer radius = 6 pixels). All data were collated and analyzed using the pandas library.

Downloaded from pubs.acs.org/jacsat/article-supplement/5420577/pdf/ja5c19089_si_001/ by guest on 21 November 2026

Fluorescently Labeling Anti-CRISPR Proteins

Synthesis of Cy5-0×NLS-Acr. An 8.3 mM stock solution of sulfo-Cyanine5 (sulfo-Cy5) maleimide (Lumiprobe, 23380) was prepared in water. 14.5 µL of the 8.3 mM sulfo-Cy5 maleimide stock solution (14.7 equiv) were added to 40 µL of 204 µM 0×NLS-Acr (1 equiv) in 20 mM Tris–HCl buffer, pH 7.5, containing 150 mM NaCl, 1 mM TCEP, and 5% v/v glycerol. The reaction mixture was gently shaken (80 RPM) for 30 min at 22 °C. Afterward, the reaction mixture was passed through a 0.5 mL Zeba spin desalting column (7 kDa MWCO), and the buffer was exchanged to 20 mM HEPES–HCl buffer, pH 7.5, containing 500 mM NaCl, 1 mM TCEP, and 5% v/v glycerol.

Synthesis of Cy5-6×NLS-Acr. An 8.3 mM stock solution of sulfo-Cy5 maleimide was prepared in water. 4 µL of the 8.3 mM sulfo-Cy5 maleimide stock solution (6.9 equiv) were added to 27.8 µL of 172 µM 6×NLS-Acr (1 equiv) in 20 mM HEPES–HCl buffer, pH 7.5, containing 500 mM NaCl, 1 mM TCEP, and 5% v/v glycerol. The reaction mixture was gently shaken (80 RPM) for 30 min at 22 °C. Afterward, the reaction mixture was passed through a 0.5 mL Zeba spin desalting column (7 kDa MWCO), and the buffer was exchanged to 20 mM HEPES–HCl buffer, pH 7.5, containing 500 mM NaCl, 1 mM TCEP, and 5% v/v glycerol.

Synthesis of Cy5-LF$_N$-Acr. A 6.2 mM stock solution of sulfo-Cy5 maleimide was prepared in water. 10 µL of the 6.2 mM sulfo-Cy5 maleimide stock solution (11.3 equiv) were added to 45 µL of 122 µM LF$_N$-Acr (1 equiv) in 20 mM Tris–HCl buffer, pH 7.5, containing 150 mM NaCl, 1 mM TCEP, and 5% v/v glycerol. The reaction mixture was gently shaken (80 RPM) for 30 min at 22 °C. Afterward, the reaction mixture was purified using a Pierce Microdyalisis Plate (10 kDa MWCO), and the buffer was exchanged to 20 mM Tris–HCl buffer, pH 7.5, containing 150 mM NaCl, 1 mM TCEP, and 5% v/v glycerol.

Direct Visualization of Anti-CRISPR Delivery

U2OS cells were seeded in a 96-well plate at a density of 10,000 cells per well in 100 µL of culture medium and incubated at 37 °C for approximately 18 h. INS-1E rat β-cells were seeded in an ECM-coated 96-well plate at a density of 75,000 cells per well in 100 µL of culture medium and incubated at 37 °C for approximately 24 h. Cells were then treated with Cy5-0×NLS-Acr (1.5–4 µM), Cy5-6×NLS-Acr (1.5–4 µM), and Cy5-LF$_N$-Acr (2.5 µM) ± PA (20 nM), and incubated for 5 min to 2 h at 37 °C. Cells were washed with FluoroBrite DMEM. Cells were stained with Hoechst 33342 (4 µg/mL, 10 min, 37 °C) and WGA555 (2.5 µg/mL, 5 min, 22 °C) in FluoroBrite DMEM, then imaged using high-throughput confocal microscopy (60× objective) to detect fluorescence from Hoechst 33342 (blue; 405 nm excitation), WGA555 (yellow; 568 nm excitation), and Cy5 (red; 647 nm excitation). Digital phase contrast (DPC) microscopy was also performed. Images were analyzed using Revvity Harmony Software. Cells were selected based on the Hoechst 33343 nuclear stain, and the cell region was defined using the WGA555 cell membrane stain. The cytoplasmic region was defined as the difference between the cell and nuclear regions. Cy5 fluorescence intensity was quantified in the nucleus (I_N) and cytoplasm (I_C) regions to determine the nuclear-to-cytoplasmic intensity ratio (I_N/I_C). Each well was imaged at more than 15 fields of view, and all imaged fields were included in the quantitative analysis. For clarity, only one representative field of view per well is shown in the figures.

Downloaded from pubs.acs.org/jacsat/article-supplement/5420577/pdf/ja5c19089_si_001/ by guest on 21 November 2026

Supplementary Tables

Table S1. Compilation of IC_{50} and Efficacy Values

Inhibitor	Dosing time (h)	End point (h)	Assay	Cell type	Figure	IC_{50} (nM)[a]	Efficacy (%)[a]
6×NLS-Acr	0	48	*GFP*	U2OS-EGFP	2B, S20	470	96
6×NLS-Acr	2	48	*GFP*	U2OS-EGFP	2B	1,460	86
LF_N-Acr	0	48	*GFP*	U2OS-EGFP	S20	2.9	86
6×NLS-Acr	0	24	HiBiT	HUES 8	S21	630	99
LF_N-Acr	0	24	HiBiT	HUES 8	S21	3.1	88
6×NLS-Acr	0	30	*GFP*	U2OS-EGFP	S32	560	99
Cy5-6×NLS-Acr	0	30	*GFP*	U2OS-EGFP	S32	670	93

[a]The "Absolute IC_{50}, X is log(concentration)" function in GraphPad Prism software was used to fit the data from the *GFP*-disruption and HiBiT-knock-in assays to determine IC_{50} and maximum Cas9 inhibition values. The maximum Cas9 inhibition value or efficacy was calculated as 100 minus the 'Bottom' value of the fitted curve, where 'Bottom' represents the baseline Cas9 activity, which approaches zero with increasing Acr concentration.

Table S2. Nuclear-to-Cytoplasmic Cy5 Intensity Ratios (I_N/I_C) for Cy5-6×NLS-Acr

Acr	[Acr] (μM)	+ Additive	*T* (°C)	Time	Cell type	Figure	I_N/I_C ratio[a]
Cy5-6×NLS-Acr	1.5	—	37	20 min	U2OS	6B, S27	5.4
Cy5-6×NLS-Acr	1.5	—	4	20 min	U2OS	6B, S30	5.6
Cy5-6×NLS-Acr	1.5	—	37	2 h	U2OS	6C, S29	4.0
Cy5-6×NLS-Acr	1	—	37	2 h	INS-1E	S28	3.7
Cy5-6×NLS-Acr	2	—	37	2 h	INS-1E	S28	4.2
Cy5-6×NLS-Acr	4	—	37	2 h	INS-1E	S28	4.2
Cy5-6×NLS-Acr	1.5	—	37	5 min	U2OS	S29	3.5
Cy5-6×NLS-Acr	1.5	Water	37	20 min	U2OS	S31	2.8
Cy5-6×NLS-Acr	1.5	Amiloride	37	20 min	U2OS	S31	2.9
Cy5-6×NLS-Acr	1.5	Bafilomycin A1	37	20 min	U2OS	S31	2.7
Cy5-6×NLS-Acr	1.5	Chloroquine	37	20 min	U2OS	S31	7.9
Cy5-6×NLS-Acr	0.13	—	37	30 h	U2OS-EGFP	S35	0.86
Cy5-6×NLS-Acr	0.25	—	37	30 h	U2OS-EGFP	S35	0.79
Cy5-6×NLS-Acr	0.5	—	37	30 h	U2OS-EGFP	S35	0.60
Cy5-6×NLS-Acr	1	—	37	30 h	U2OS-EGFP	S35	0.53
Cy5-6×NLS-Acr	2	—	37	30 h	U2OS-EGFP	S35	0.46
Cy5-6×NLS-Acr	4	—	37	30 h	U2OS-EGFP	S35	0.42
Cy5-LF_N-Acr	2.5	—	37	2 h	U2OS	S37	0.65
Cy5-LF_N-Acr	2.5	20 nM PA	37	2 h	U2OS	S37	0.65
Cy5-LF_N-Acr	2.5	—	37	30 h	U2OS-EGFP	S40	0.56
Cy5-LF_N-Acr	2.5	20 nM PA	37	30 h	U2OS-EGFP	S40	0.59
Cy5-LF_N-Acr	0.5	—	37	30 h	U2OS-EGFP	S40	0.79
Cy5-LF_N-Acr	0.5	20 nM PA	37	30 h	U2OS-EGFP	S40	0.80

[a]Nuclear-to-cytoplasmic Cy5 fluorescence intensity ratios (I_N/I_C) were determined using Harmony image analysis software.

Downloaded from pubs.acs.org/jacsat/article-supplement/5420577/pdf/ja5c19089_si_001/ by guest on 21 November 2026

Table S3. Cell Lines Used in This Study

Cell Line	Purpose	Reference
NEB® 5-alpha Competent *E. coli* (High Efficiency)	Cloning bacterial expression vectors	NEB
Rosetta 2(DE3) Competent Cells (Novagen)	Producing and purifying Acrs	MilliporeSigma
NEB® Stable Competent *E. coli* (High Efficiency)	Cloning mammalian expression vectors	NEB
U2OS-EGFP.PEST	*GFP*-disruption assay	Reyon et al. (2012)[6]
HUES 8 (RRID:CVCL_B207)	HiBiT-knock-in assay	Harvard Stem Cell Institute (HSCI) iPS Core Facility; Cowan et al. (2004)[7]
HEK293T	HiBiT-kock-in, T7E1, and NGS assays	ATCC
U2OS-Cas9-GFP	Direct visualization of the inhibition of Cas9–GFP	Liu et al. (2020)[8]
U2OS	Direct visualization of Acr delivery	ATCC
INS-1E rat β-cells	Direct visualization of Acr delivery	Millipore Sigma

Downloaded from pubs.acs.org/jacsat/article-supplement/5420577/pdf/ja5c19089_si_001/ by guest on 21 November 2026

Table S4. Proteins Used in This Study

Protein	Source	Reference
6×NLS-Acr	Purified in-house	This work
0×NLS-Acr	Purified in-house	Vera et al. (2025)[2]
1×NLS-Acr	Purified in-house	Vera et al. (2025)[2]
LF_N-Acr	Purified in-house	Vera et al. (2025)[2]
Protective Antigen	Purified in-house	Pomerantsev et al. (2021)[9]
SpCas9-NLS	GenScript	Cat. No. Z03385
2×NLS-LbCas12a	NEB	Cat. No. M0653T
TEV protease	Purified in-house	Kapust et al. (2001)[3]

Table S5. Plasmids Used in This Study

Plasmid name	Purpose	Reference
4xNLS-pMJ915v2	Amplifying the backbone used to clone pAV13	Staahl et al. (2017)[1] Addgene #88917
pAV13-MBP-TEV-4×NLS-Cys-AcrIIA4-2×NLS	Bacterial production and purification of 6×NLS-Acr	This work
pAV17-MBP-TEV-Cys-AcrIIA4	Bacterial production and purification of 0×NLS-Acr	Vera et al. (2025)[2]
pAV18-MBP-TEV-Cys-AcrIIA4-NLS	Bacterial production and purification of 1×NLS-Acr	Vera et al. (2025)[2]
pAV14-MBP-TEV-LF_N-Cys-AcrIIA4-NLS	Bacterial production and purification of LF_N-Acr	Vera et al. (2025)[2]
pYS5-PA BH500	Bacterial production and purification of PA	Singh et al. (1989)[10]
pRK793	Bacterial production and purification of TEV protease	Kapust et al. (2001)[3] Addgene #8827
pX330-U6-Chimeric_BB-CBh-hSpCas9	Mammalian production of 2×NLS-SpCas9	Cong et al. (2013)[4] Addgene #42230
JDS246	Mammalian production of SpCas9-NLS	Addgene #43861
pEMX1-gRNA	Mammalian production of EMX1 gRNA	Sreekanth et al. (2020)[5]

Downloaded from pubs.acs.org/jacsat/article-supplement/5420577/pdf/ja5c19089_si_001/ by guest on 21 November 2026

Table S6. Primer Sequences for gRNA Cloning and Synthesis for RNP Experiments

Primer	Sequence[a]
GFP Fwd	TAATACGACTCACTATA**GGTGGTGCAGATGAACTTCA**GTTTTAGAGCTAGAAAT
GAPDH Fwd	TAATACGACTCACTATA**GGTCCAGGGGTCTTACTCCT**GTTTTAGAGCTAGAAAT
Universal Rev	AAAAGCACCGACTCGGTGCCACTTTTTCAAGTTGATAACGGACTAGCCTTATTTT AACTTGCTATTTCTAGCTCTAAAAC

[a]The spacer sequence is in bold typeface.

Table S7. Sequence[a] of the LbCas12a crRNA Used in the *GFP*-Disruption Assay

LbCas12a crRNA	UAAUUUCUACUAAGUGUAGAU**CGUCGCCGUCCAGCUCGACCAGG**

[a]The spacer sequence is in bold typeface. LbCas12a crRNA was ordered from IDT.

Table S8. ssODN Sequence

GAPDH HiBiT	TCTTCTAGGTATGACAACGAATTTGGCTACAGCAACAGGGTGGTGGACCTCATGGCCCACA TGGCCTCCAAGGAGGTGAGCGGCTGGCGGCTGTTCAAGAAGATTAGCTAAGACCCCTGGAC CACCAGCCCCAGCAAGAGCACAAGAGGAAGAGAGAGACCCTCACTGCTGGGGAGTCCCTGC

Table S9. Spacer Sequence of Plasmid-Encoded EMX1 gRNA

EMX1	GAGTCCGAGCAGAAGAAGAA

Downloaded from pubs.acs.org/jacsat/article-supplement/5420577/pdf/ja5c19089_si_001/ by guest on 21 November 2026

Table S10. Primers Used to Generate Amplicons for Next-Generation Sequencing

	Target	PAM	Forward Primer	Reverse Primer
EMX1 On	GAGTCCGAGCAG AAGAAGAA	GGG	ACACTCTTTCCCTACACGA CGCTCTTCCGATCTNNNNC AGCTCAGCCTGAGTGTTGA	TGGAGTTCAGACGTGTGCT CTTCCGATCTCTCGTGGGT TTGTGGTTGC
EMX1 OT1	GAGTTAGAGCAG AAGAAGAA	AGG	ACACTCTTTCCCTACACGA CGCTCTTCCGATCTNNNNT TCTGAGGGCTGCTACCTGT	TGGAGTTCAGACGTGTGCT CTTCCGATCTGCCCAATCA TTGATGCTTTT
EMX1 OT2	GAGTCTAAGCAG AAGAAGAA	GAG	ACACTCTTTCCCTACACGA CGCTCTTCCGATCTNNNNC ACGGCCTTTGCAAATAGAG	TGGAGTTCAGACGTGTGCT CTTCCGATCTGGCTTTCAC AAGGATGCAGT
EMX1 OT3	AAGTCTGAGCAC AAGAAGAA	TGG	ACACTCTTTCCCTACACGA CGCTCTTCCGATCTNNNNG TTCTGACATTCCTCCTGAG GGA	TGGAGTTCAGACGTGTGCT CTTCCGATCTATGGCTTAC ATATTTATTAGATAAAATG TATTCC
EMX1 OT4	GAGTCCTAGCAG GAGAAGAA	GAG	ACACTCTTTCCCTACACGA CGCTCTTCCGATCTNNNNC CAGACTCAGTAAAGCCTGG A	TGGAGTTCAGACGTGTGCT CTTCCGATCTTGGCCCCAG TCTCTCTTCTA

Downloaded from pubs.acs.org/jacsat/article-supplement/5420577/pdf/ja5c19089_si_001/ by guest on 21 November 2026

Table S11. Amplicon Sequences

Target	Sequence
EMX1 On	CAGCTCAGCCTGAGTGTTGAGGCCCCAGTGGCTGCTCTGGGGGCCTCCTGAGTTTCTC ATCTGTGCCCCTCCCTCCCTGGCCCAGGTGAAGGTGTGGTTCCAGAACCGGAGGACAA AGTACAAACGGCAGAAGCTGGAGGAGGAAGGGCCTGAGTCCGAGCAGAAGAAGAAGGG CTCCCATCACATCAACCGGTGGCGCATTGCCACGAAGCAGGCCAATGGGGAGGACATC GATGTCACCTCCAATGACTAGGGTGGGCAACCACAAACCCACGAG
EMX1 OT1	TTCTGAGGGCTGCTACCTGTACATCTGCACAAGATTGCCTTTACTCCATGCCTTTCTT CTTCTGCTCTAACTCTGACAATCTGTCTTGCCATGCCATAAGCCCCTATTCTTTCTGT AACCCCAAGATGGTATAAAAGCATCAATGATTGGGC
EMX1 OT2	CACGGCCTTTGCAAATAGAGCCCTTTATTCATAGTAGACAAGAGTCTAAGCAGAAGAA GAAGAGAGCCACTACCCAACCATCTACTCTTCTAATGGTGTTTTCCTACAAAGGCCAA GTCATGAGACTGCATCCTTGTGAAAGCC
EMX1 OT3	GTTCTGACATTCCTCCTGAGGGAAAATAAATAAATTAATTAAAAATATATATATATAT GTATAATGATAAACATGCTAACAAAGTCTGAGCACAAGAAGAATGGTGAGAAGGAATA CATTTTATCTAATAAATATGTAAGCCAT
EMX1 OT4	CCAGACTCAGTAAAGCCTGGAGGCTGCCAGGTAGGGCTGGGGCCAGCATGACCTGAGT CCTAGCAGGAGAAGAAGAGGCAGCCTAGAGTCTTCTGTGAAGTGCACATAGAAGAGAG ACTGGGGCCA

Table S12. Sequence[a] of Truncated Ch3Rep gRNA

Ch3Rep gRNA	G**UGAUAUCACAG**GUUUUAGAGCUAGAAAUAGCAAGUUAAAAUAAGGCUAGUCCGUUAUCA ACUUGAAAAAGUGGCACCGAGUCGGUGCUUUU

[a]The truncated spacer sequence is in bold typeface.

Downloaded from pubs.acs.org/jacsat/article-supplement/5420577/pdf/ja5c19089_si_001/ by guest on 21 November 2026

Supplementary Figures

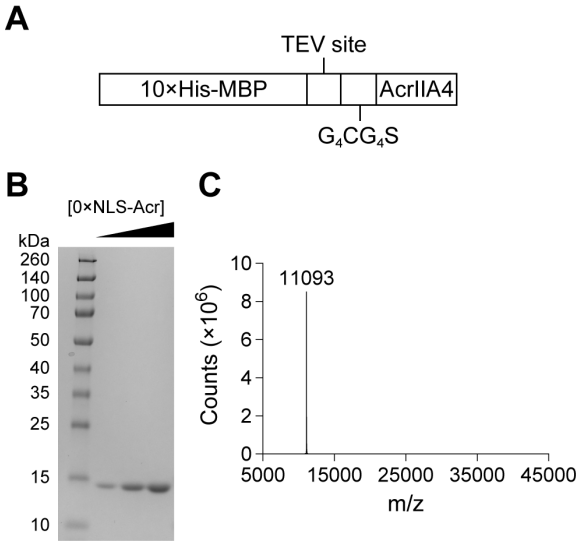


Figure S1. Purification of 0×NLS-Acr. (A) The construct that was used to produce and purify 0×NLS-Acr (pAV17-MBP-TEV-Cys-AcrIIA4). A protein fusion between a polyhistidine-tagged maltose-binding protein (10×His-MBP, for solubility and purification), a TEV protease cleavage site, a glycine–cysteine–serine linker (G_4CG_4S, for flexibility and optional bioconjugation), and AcrIIA4 (for Cas9 inhibition). (B) Assessing 0×NLS-Acr purity by SDS–PAGE. The concentration of 0×NLS-Acr increases from left to right. (C) Assessing 0×NLS-Acr purity by Q-TOF LC–MS.

Downloaded from pubs.acs.org/jacsat/article-supplement/5420577/pdf/ja5c19089_si_001/ by guest on 21 November 2026

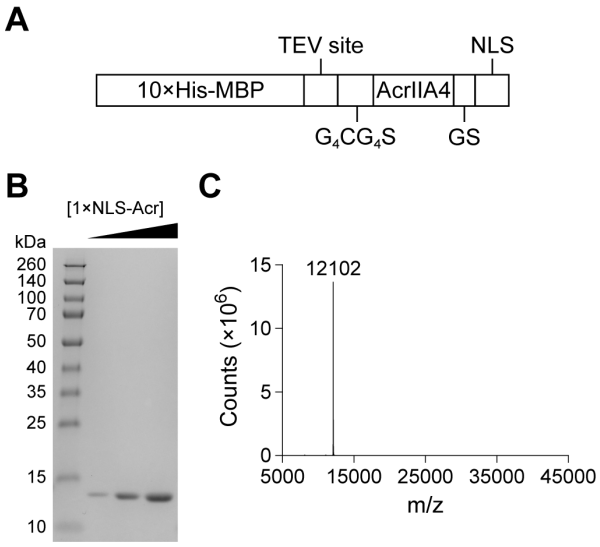


Figure S2. Purification of 1×NLS-Acr. (A) The construct that was used to produce and purify 1×NLS-Acr (pAV18-MBP-TEV-Cys-AcrIIA4-NLS). A protein fusion between a 10×His-MBP tag, a TEV protease cleavage site, a G_4CG_4S linker, AcrIIA4, a GS linker (for flexibility), and an SV40 nuclear localization signal (NLS). (B) Assessing 1×NLS-Acr purity by SDS–PAGE. The concentration of 1×NLS-Acr increases from left to right. (C) Assessing 1×NLS-Acr purity by Q-TOF LC–MS.

Downloaded from pubs.acs.org/jacsat/article-supplement/5420577/pdf/ja5c19089_si_001/ by guest on 21 November 2026

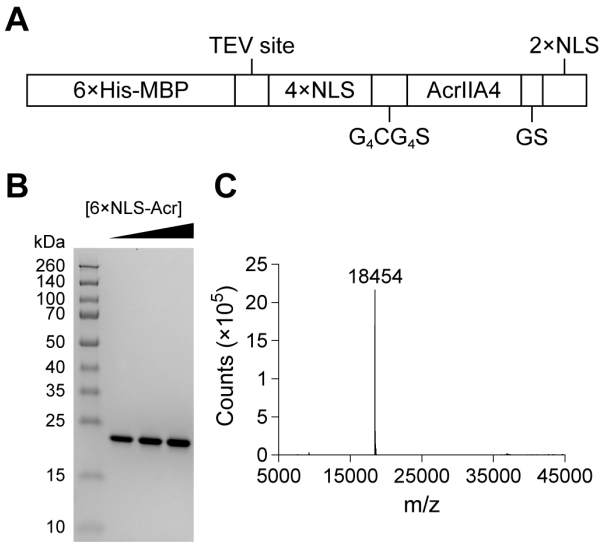


Figure S3. Purification of 6×NLS-Acr. (A) The construct that was used to produce and purify 6×NLS-Acr (pAV13-MBP-TEV-6×NLS-AcrIIA4). A protein fusion between a 6×His-MBP tag, a TEV protease cleavage site, a 4×NLS tag (for cellular delivery and nuclear localization), a G_4CG_4S linker, AcrIIA4, a GS linker, and a 2×NLS tag (for cellular delivery and nuclear localization). (B) Assessing 6×NLS-Acr purity by SDS–PAGE. The concentration of 6×NLS-Acr increases from left to right. (C) Assessing 6×NLS-Acr purity by Q-TOF LC–MS.

Downloaded from pubs.acs.org/jacsat/article-supplement/5420577/pdf/ja5c19089_si_001/ by guest on 21 November 2026

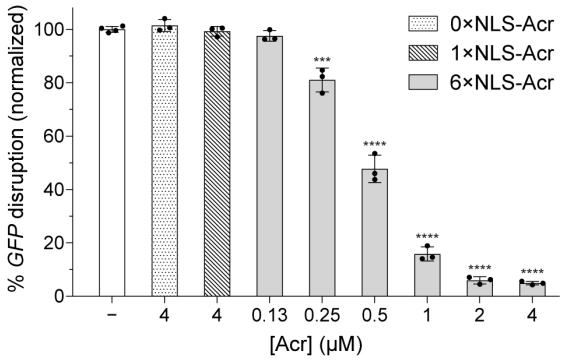


Figure S4. Dose-dependent inhibition of Cas9 by 6×NLS-Acr in the *GFP*-disruption assay (0-h dosing time). SpCas9-NLS RNP (20 pmol) targeting *GFP* was delivered via nucleofection into U2OS-EGFP.PEST cells. The cells were seeded, incubated at 37 °C, and treated with 6×NLS-Acr (0.13–4 μM) at 0 h. After 48 h, live cells were stained with Hoechst 33342 and imaged using high-throughput confocal microscopy. Controls include nucleofection of Cas9 RNP (white bar) and nucleofection of Cas9 RNP followed by treatment with 0×NLS-Acr (4 μM) or 1×NLS-Acr (4 μM) at 0 h. The values were normalized to Cas9 RNP and are the mean ± standard deviation (SD) of three independent replicates. The significance of 6×NLS-Acr delivery was determined with an unpaired, two-tailed *t*-test versus Cas9 RNP, where *, **, ***, and **** refer to $P \leq 0.05$, $P \leq 0.01$, $P \leq 0.001$, and $P \leq 0.0001$, respectively.

Downloaded from pubs.acs.org/jacsat/article-supplement/5420577/pdf/ja5c19089_si_001/ by guest on 21 November 2026

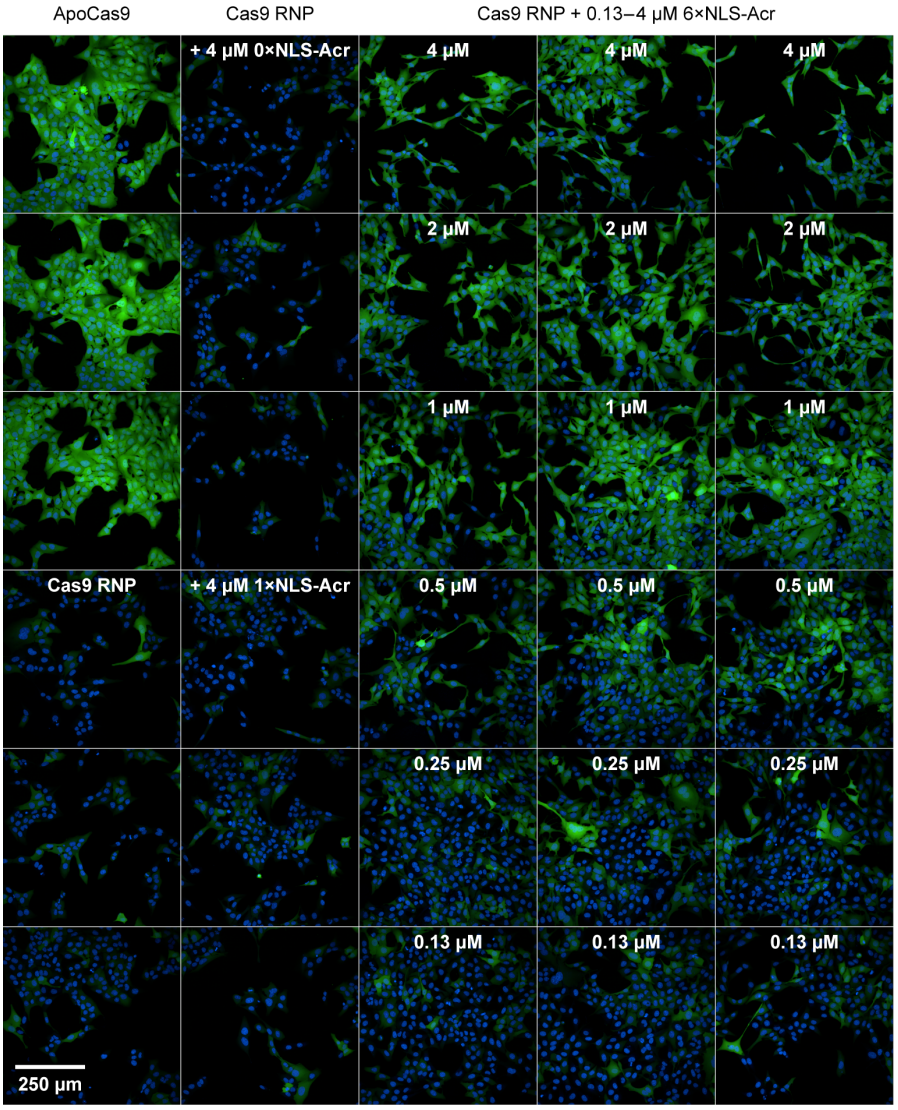


Figure S5. Representative fluorescence images from the *GFP*-disruption assay in Figure S4. SpCas9-NLS RNP (20 pmol) targeting *GFP* was delivered via nucleofection into U2OS-EGFP.PEST cells. The cells were seeded, incubated at 37 °C, and treated with 6×NLS-Acr (0.13–4 μM) at 0 h. After 48 h, live cells were stained with Hoechst 33342 (blue, nucleus) and imaged using high-throughput confocal microscopy. Controls include nucleofection of Apo-Cas9, nucleofection of Cas9 RNP, and nucleofection of Cas9 RNP followed by treatment with 0×NLS-Acr (4 μM) or 1×NLS-Acr (4 μM) at 0 h.

Downloaded from pubs.acs.org/jacsat/article-supplement/5420577/pdf/ja5c19089_si_001/ by guest on 21 November 2026

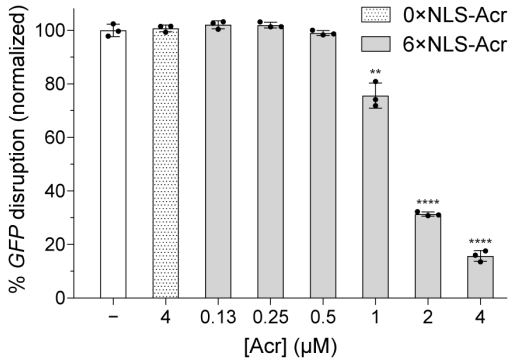


Figure S6. Dose-dependent inhibition of Cas9 by 6×NLS-Acr in the *GFP*-disruption assay (2-h dosing time). SpCas9-NLS RNP (20 pmol) targeting *GFP* was delivered via nucleofection into U2OS-EGFP.PEST cells. The cells were seeded, incubated at 37 °C, and treated with 6×NLS-Acr (0.13–4 μM) at 2 h. After 48 h, live cells were stained with Hoechst 33342 and imaged using high-throughput confocal microscopy. Controls include nucleofection of Cas9 RNP (white bar) and nucleofection of Cas9 RNP followed by treatment with 0×NLS-Acr (4 μM) at 2 h. The values were normalized to Cas9 RNP and are the mean ± SD of three independent replicates. The significance of 6×NLS-Acr delivery was determined with an unpaired, two-tailed *t*-test versus Cas9 RNP, where *, **, ***, and **** refer to $P \leq 0.05$, $P \leq 0.01$, $P \leq 0.001$, and $P \leq 0.0001$, respectively.

Downloaded from pubs.acs.org/jacsat/article-supplement/5420577/pdf/ja5c19089_si_001/ by guest on 21 November 2026

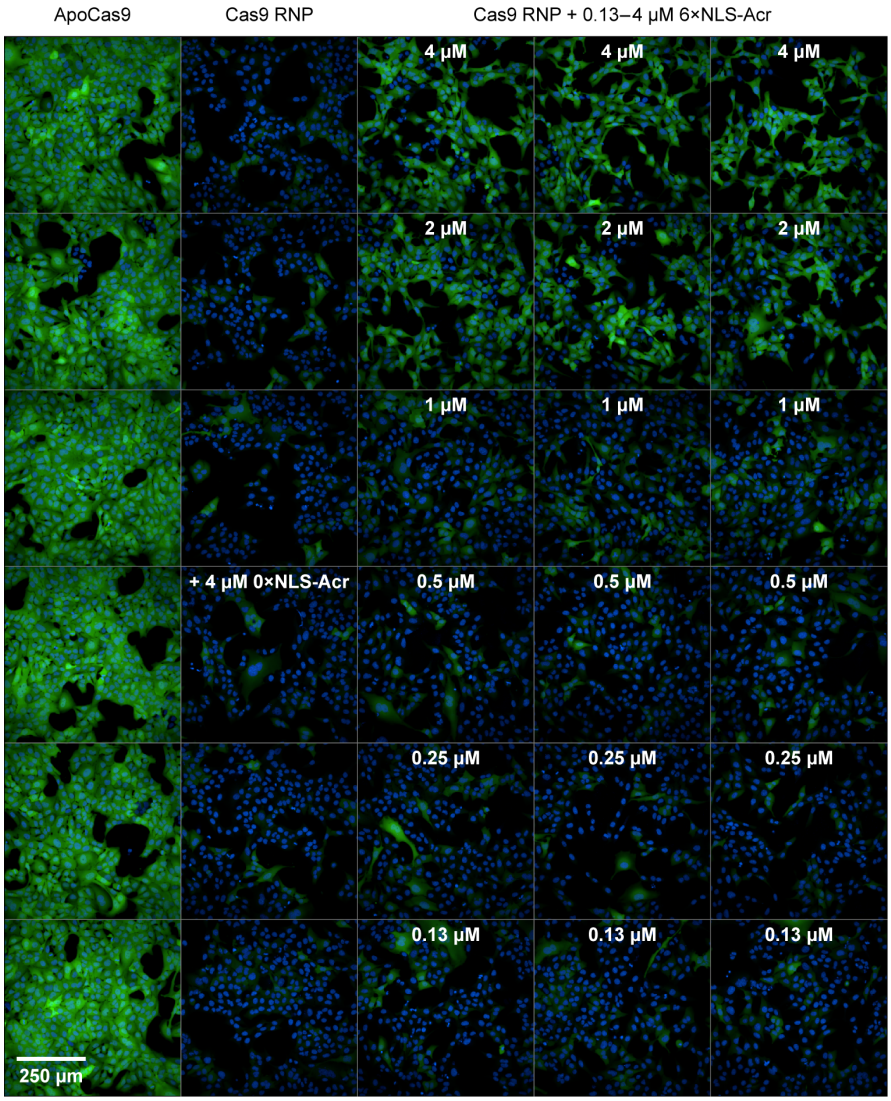


Figure S7. Representative fluorescence images from the *GFP*-disruption assay in Figure S6. SpCas9-NLS RNP (20 pmol) targeting *GFP* was delivered via nucleofection into U2OS-EGFP.PEST cells. The cells were seeded, incubated at 37 °C, and treated with 6×NLS-Acr (0.13–4 μM) at 2 h. After 48 h, live cells were stained with Hoechst 33342 (blue, nucleus) and imaged using high-throughput confocal microscopy. Controls include nucleofection of Apo-Cas9, nucleofection of Cas9 RNP, and nucleofection of Cas9 RNP followed by treatment with 0×NLS-Acr (4 μM) at 2 h.

Downloaded from pubs.acs.org/jacsat/article-supplement/5420577/pdf/ja5c19089_si_001/ by guest on 21 November 2026

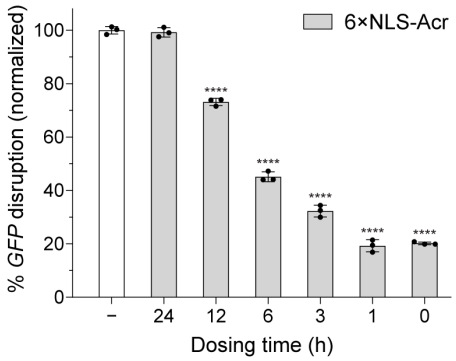


Figure S8. Time-dependent inhibition of Cas9 by 6×NLS-Acr in the *GFP*-disruption assay. SpCas9-NLS RNP (20 pmol) targeting *GFP* was delivered via nucleofection into U2OS-EGFP.PEST cells. The cells were seeded, incubated at 37 °C, and treated with 6×NLS-Acr (1 μM), varying the dosing time from 0 to 24 h. After 48 h, live cells were stained with Hoechst 33342 and imaged using high-throughput confocal microscopy. Nucleofection of Cas9 RNP (white bar) serves as the control. The values were normalized to Cas9 RNP and are the mean ± SD of three independent replicates. The significance of 6×NLS-Acr delivery was determined with an unpaired, two-tailed *t*-test versus Cas9 RNP, where *, **, ***, and **** refer to $P \leq 0.05$, $P \leq 0.01$, $P \leq 0.001$, and $P \leq 0.0001$, respectively.

Downloaded from pubs.acs.org/jacsat/article-supplement/5420577/pdf/ja5c19089_si_001/ by guest on 21 November 2026

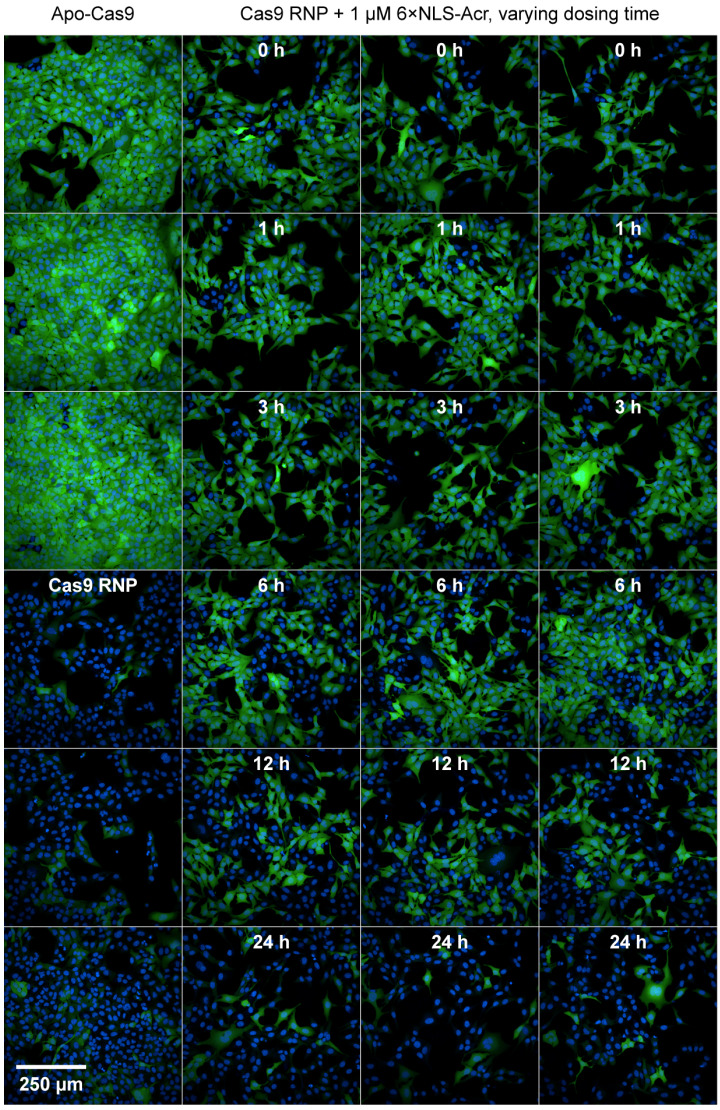


Figure S9. Representative fluorescence images from the *GFP*-disruption assay in Figure S8. SpCas9-NLS RNP (20 pmol) targeting *GFP* was delivered via nucleofection into U2OS-EGFP.PEST cells. The cells were seeded, incubated at 37 °C, and treated with 6×NLS-Acr (1 μM), varying the dosing time from 0 to 24 h. After 48 h, live cells were stained with Hoechst 33342 (blue, nucleus) and imaged using high-throughput confocal microscopy. Nucleofection of Cas9 RNP (white bar) serves as the control.

Downloaded from pubs.acs.org/jacsat/article-supplement/5420577/pdf/ja5c19089_si_001/ by guest on 21 November 2026

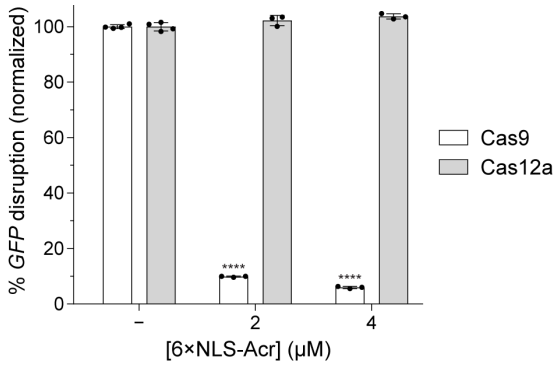


Figure S10. Effect of 6×NLS-Acr delivery on Cas protein activity in human cells. SpCas9-NLS (20 pmol) or 2×NLS-LbCas12a (20 pmol) RNP targeting *GFP* was delivered via nucleofection into U2OS-EGFP.PEST cells. The cells were seeded, incubated at 37 °C, and treated with 6×NLS-Acr (2–4 μM) at 0 h. After 48 h, live cells were stained with Hoechst 33342 and imaged using high-throughput confocal microscopy. Controls include nucleofection of Cas9 RNP (−, white bar) and nucleofection of Cas12a RNP (−, gray bar). The values were normalized to Cas9 RNP (white bars) or Cas12a RNP (gray bars) and are the mean ± SD of three independent replicates. The significance of 6×NLS-Acr delivery was determined with an unpaired, two-tailed *t*-test versus Cas9 RNP (white bars) or Cas12a RNP (gray bars), where *, **, ***, and **** refer to $P \leq 0.05$, $P \leq 0.01$, $P \leq 0.001$, and $P \leq 0.0001$, respectively.

Downloaded from pubs.acs.org/jacsat/article-supplement/5420577/pdf/ja5c19089_si_001/ by guest on 21 November 2026

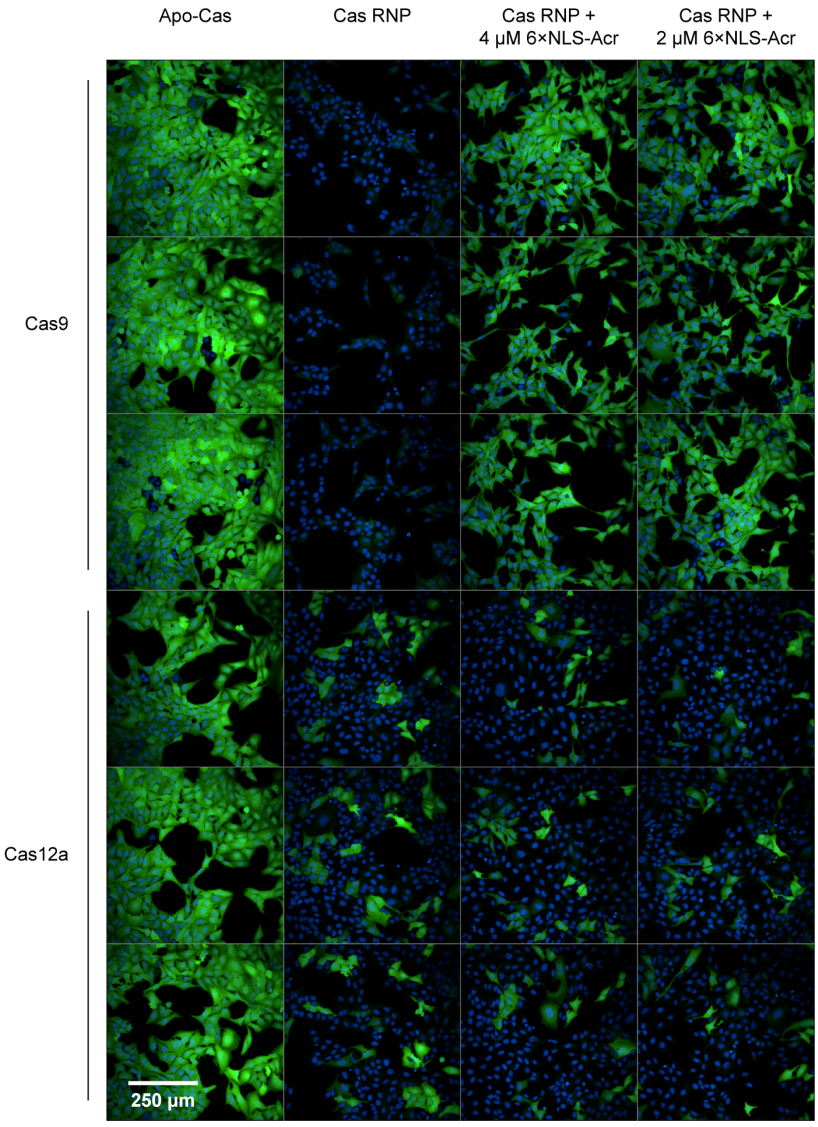


Figure S11. Representative fluorescence images from the *GFP*-disruption assay in Figure S10. SpCas9-NLS (20 pmol) or 2×NLS-LbCas12a (20 pmol) RNP targeting *GFP* was delivered via nucleofection into U2OS-EGFP.PEST cells. The cells were seeded, incubated at 37 °C, and treated with 6×NLS-Acr (2–4 μM) at 0 h. After 48 h, live cells were stained with Hoechst 33342 (blue, nucleus) and imaged using high-throughput confocal microscopy. Controls include nucleofection of Apo-Cas proteins and nucleofection of Cas RNPs.

Downloaded from pubs.acs.org/jacsat/article-supplement/5420577/pdf/ja5c19089_si_001/ by guest on 21 November 2026

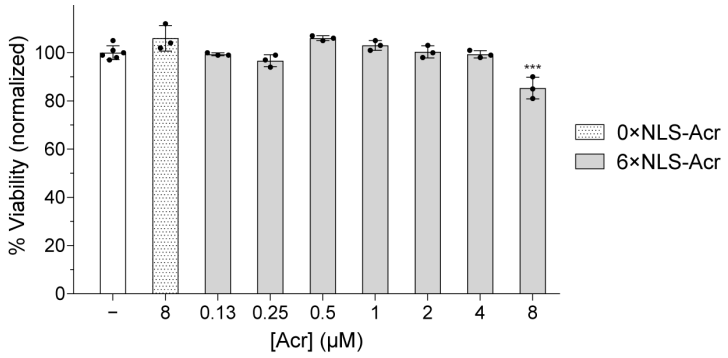


Figure S12. Cell viability of U2OS-EGFP.PEST cells after 6×NLS-Acr delivery. U2OS-EGFP.PEST cells were seeded, incubated at 37 °C, and treated with 6×NLS-Acr (0.13–8 μM) at 2 h. After 24 h, the cells were incubated with the CellTiter-Glo reagent and lysed. Cell viability was determined using luminescence. Controls include cells treated with buffer (white bar) or 0×NLS-Acr (8 μM) at 2 h. The values were normalized to the buffer-only treatment and are the mean ± SD of three independent replicates. The significance of 6×NLS-Acr delivery was determined with an unpaired, two-tailed *t*-test versus the buffer-only treatment.

Downloaded from pubs.acs.org/jacsat/article-supplement/5420577/pdf/ja5c19089_si_001/ by guest on 21 November 2026

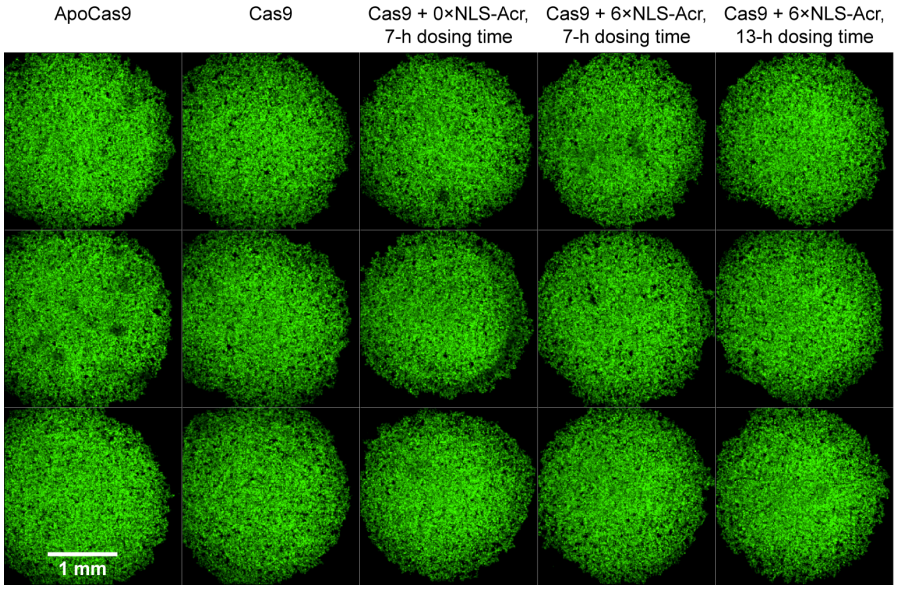


Figure S13. Fluorescence imaging shows loosely aggregated spheroids forming 7 h after cell seeding. SpCas9-NLS RNP (20 pmol) targeting *GFP* was delivered via nucleofection into U2OS-EGFP.PEST cells. The cells were seeded in a spheroid plate and incubated at 37 °C. After 7 h, live cells were imaged using high-throughput confocal microscopy. Controls include nucleofection of Apo-Cas9 and nucleofection of Cas9 RNP. Each column is labeled with the Acr that was eventually added to the 3D cell culture. However, these images were captured immediately before treating cells with Acrs at 7 h to show the appearance of the 3D cell cultures at the 7-h dosing time. The images represent maximum intensity projections from a Z-stack. The average diameter of the loosely aggregated spheroids is 2.53 ± 0.08 mm. Although *GFP* disruption has started by 7 h, the loosely aggregated spheroids appear equally fluorescent because GFP protein has not yet degraded.

Downloaded from pubs.acs.org/jacsat/article-supplement/5420577/pdf/ja5c19089_si_001/ by guest on 21 November 2026

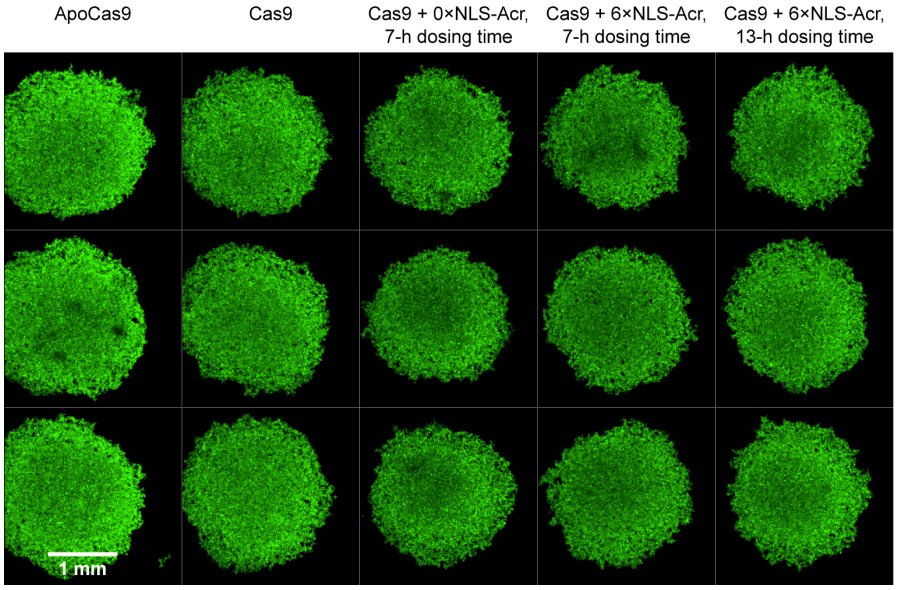


Figure S14. Fluorescence imaging shows loosely aggregated spheroids forming 13 h after cell seeding. SpCas9-NLS RNP (20 pmol) targeting *GFP* was delivered via nucleofection into U2OS-EGFP.PEST cells. The cells were seeded in a spheroid plate and incubated at 37 °C. After 13 h, live cells were imaged using high-throughput confocal microscopy. Controls include nucleofection of Apo-Cas9, nucleofection of Cas9 RNP, and nucleofection of Cas9 RNP followed by treatment with 0×NLS-Acr (2.5 μM) at 7 h. Each column is labeled with the Acr that was eventually added to the 3D cell culture. However, these images were captured immediately before treating cells with 6×NLS-Acr at 13 h to show the appearance of the 3D cell cultures at the 13-h dosing time. The images represent maximum intensity projections from a Z-stack. The average diameter of the loosely aggregated spheroids is 2.10 ± 0.08 mm. Although *GFP* disruption has started by 13 h, the loosely aggregated spheroids appear equally fluorescent because GFP protein has not yet degraded. These are the same cells imaged in Figure S13 but at a later time point (13 h).

Downloaded from pubs.acs.org/jacsat/article-supplement/5420577/pdf/ja5c19089_si_001/ by guest on 21 November 2026

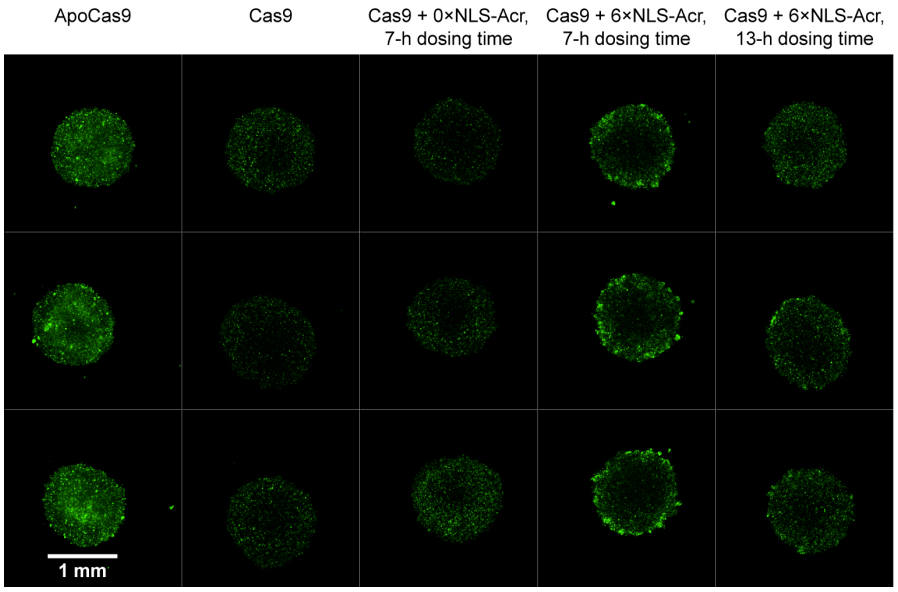


Figure S15. Representative fluorescence images from the *GFP*-disruption assay in Figure S16. SpCas9-NLS RNP (20 pmol) targeting *GFP* was delivered via nucleofection into U2OS-EGFP.PEST cells. The cells were seeded in a spheroid plate, incubated at 37 °C, and treated with 6×NLS-Acr (2.5 μM) at 7 and 13 h. After 48 h, live cells were imaged using high-throughput confocal microscopy. Controls include nucleofection of Apo-Cas9, nucleofection of Cas9 RNP, and nucleofection of Cas9 RNP followed by treatment with 0×NLS-Acr (2.5 μM) at 7 h. The images represent maximum intensity projections from a Z-stack. The approximate diameter of these well-defined spheroids is 1.25 ± 0.05 mm. These are the same cells imaged in Figures S13 and S14, but at a later time point (48 h).

Downloaded from pubs.acs.org/jacsat/article-supplement/5420577/pdf/ja5c19089_si_001/ by guest on 21 November 2026

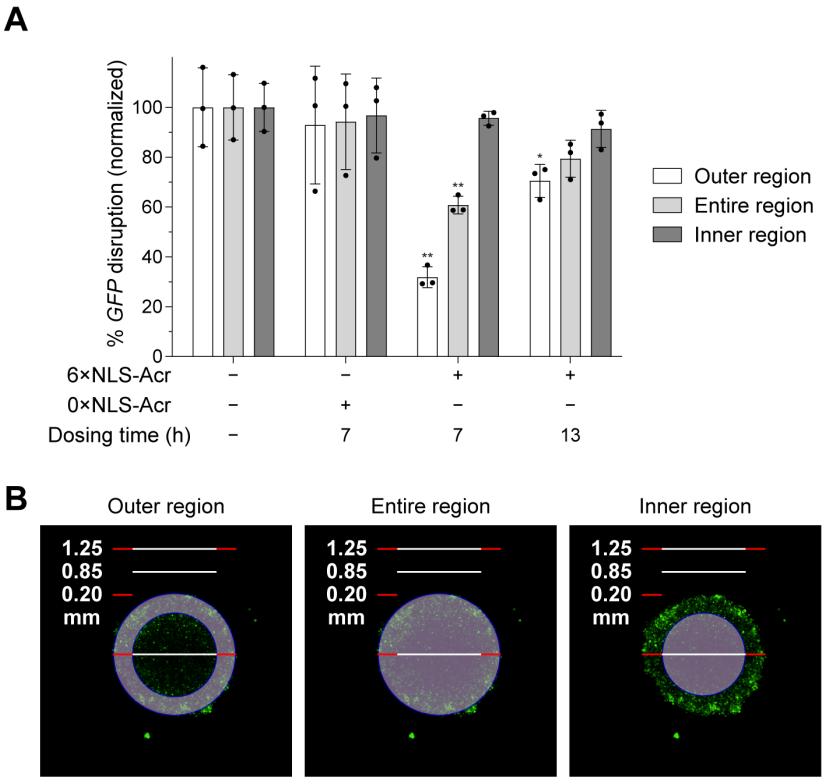


Figure S16. Effect of 6×NLS-Acr delivery on Cas9 activity in the different layers of the spheroid. (A) SpCas9-NLS RNP (20 pmol) targeting *GFP* was delivered via nucleofection into U2OS-EGFP.PEST cells. The cells were seeded in a spheroid plate, incubated at 37 °C, and treated with 6×NLS-Acr (2.5 μM) at 7 and 13 h. After 48 h, live cells were imaged using high-throughput confocal microscopy. Controls include nucleofection of Cas9 RNP (−, dosing time) and nucleofection of Cas9 RNP followed by treatment with 0×NLS-Acr (2.5 μM) at 7 h. White bars show *GFP* disruption in the outer spheroid region (the area that is 0.20 mm in depth). Light gray bars show *GFP* disruption in the entire spheroid region, which has an average diameter of 1.25 mm. Dark gray bars show *GFP* disruption in the inner spheroid region (the area that is 0.85 mm in diameter). The values were normalized to Cas9 RNP for each region and are the mean ± SD of three independent replicates. The significance of 6×NLS-Acr delivery was determined with an unpaired, two-tailed *t*-test versus Cas9 RNP for each region, where *, **, ***, and **** refer to $P \leq 0.05$, $P \leq 0.01$, $P \leq 0.001$, and $P \leq 0.0001$, respectively. (B) Visual representation of the spheroid regions defined to quantify *GFP* disruption in panel A. Each region (outer, entire, and inner region) is shaded in light purple. 6×NLS-Acr delivery at 7 and 13 h reduced *GFP* disruption in the outer spheroid region.

Downloaded from pubs.acs.org/jacsat/article-supplement/5420577/pdf/ja5c19089_si_001/ by guest on 21 November 2026

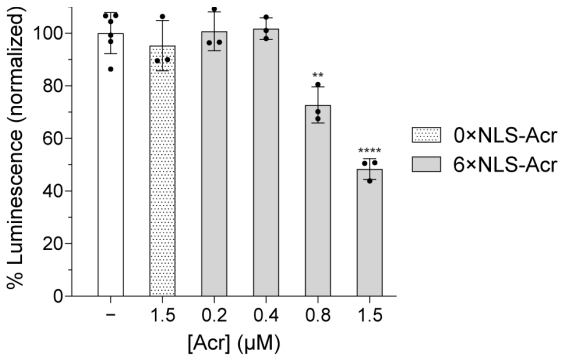


Figure S17. Dose-dependent inhibition of Cas9 by 6×NLS-Acr in the HiBiT-knock-in assay (HEK293T cells). SpCas9-NLS RNP (20 pmol) targeting *GAPDH* and the HiBiT ssODN (80 pmol) were co-delivered via nucleofection into HEK293T cells. The cells were seeded, incubated at 37 °C, and treated with 6×NLS-Acr (0.2–1.5 μM) at 0 h. After 72 h, the cells were lysed and combined with LgBiT and furimazine, and their luminescence was quantified. Controls include co-nucleofection of Cas9 RNP and ssODN (white bar) and co-nucleofection of Cas9 RNP and ssODN followed by treatment with 0×NLS-Acr (1.5 μM) at 0 h. The values were normalized to Cas9 RNP with ssODN and are the mean ± SD of three independent replicates. The significance of 6×NLS-Acr delivery was determined with an unpaired, two-tailed *t*-test versus Cas9 RNP with ssODN, where *, **, ***, and **** refer to $P \leq 0.05$, $P \leq 0.01$, $P \leq 0.001$, and $P \leq 0.0001$, respectively.

Downloaded from pubs.acs.org/jacsat/article-supplement/5420577/pdf/ja5c19089_si_001/ by guest on 21 November 2026

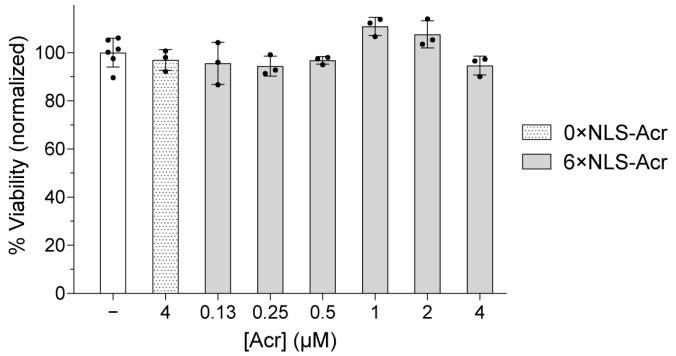


Figure S18. Cell viability after 6×NLS-Acr delivery in the HiBiT-knock-in assay (HUES 8 cells). SpCas9-NLS RNP (20 pmol) targeting *GAPDH* and the HiBiT ssODN (80 pmol) were co-delivered via nucleofection into HUES 8 cells. The cells were seeded, incubated at 37 °C, and treated with 6×NLS-Acr (0.13–4 μM) at 0 h. After 24 h, the cells were incubated with the PrestoBlue HS reagent. Cell viability was determined using fluorescence spectroscopy (560 nm excitation/590 nm emission). Controls include co-nucleofection of Cas9 RNP and ssODN (white bar) and co-nucleofection of Cas9 RNP and ssODN followed by treatment with 0×NLS-Acr (4 μM) at 0 h. The values were normalized to Cas9 RNP with ssODN and are the mean ± SD of three independent replicates. The significance of 6×NLS-Acr delivery was determined with an unpaired, two-tailed *t*-test versus Cas9 RNP with ssODN. No statistically significant decreases in viability were detected.

Downloaded from pubs.acs.org/jacsat/article-supplement/5420577/pdf/ja5c19089_si_001/ by guest on 21 November 2026

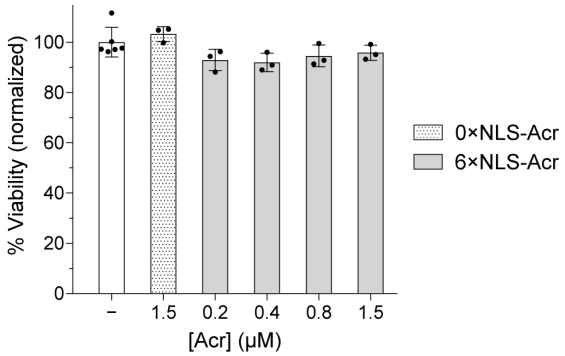


Figure S19. Cell viability after 6×NLS-Acr delivery in the HiBiT-knock-in assay (HEK293T cells). SpCas9-NLS RNP (20 pmol) targeting *GAPDH* and the HiBiT ssODN (80 pmol) were co-delivered via nucleofection into HEK293T cells. The cells were seeded, incubated at 37 °C, and treated with 6×NLS-Acr (0.2–1.5 μM) at 0 h. After 72 h, the cells were incubated with the PrestoBlue HS reagent. Cell viability was determined using fluorescence spectroscopy (560 nm excitation/590 nm emission). Controls include co-nucleofection of Cas9 RNP and ssODN (white bar) and co-nucleofection of Cas9 RNP and ssODN followed by treatment with 0×NLS-Acr (1.5 μM) at 0 h. The values were normalized to Cas9 RNP with ssODN and are the mean ± SD of three independent replicates. The significance of 6×NLS-Acr delivery was determined with an unpaired, two-tailed *t*-test versus Cas9 RNP with ssODN. No statistically significant decreases in viability were detected.

Downloaded from pubs.acs.org/jacsat/article-supplement/5420577/pdf/ja5c19089_si_001/ by guest on 21 November 2026

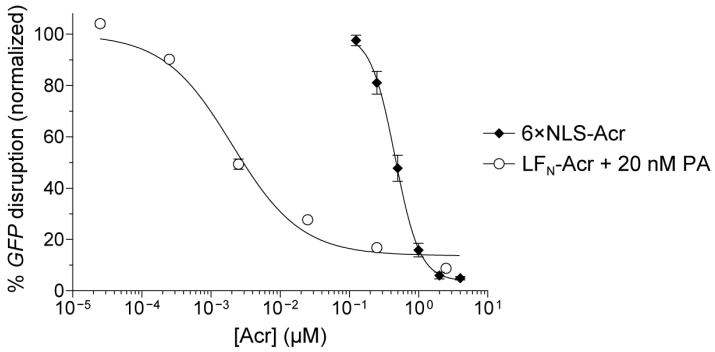


Figure S20. Dose-dependent inhibition of Cas9 by 6×NLS-Acr and LF_N-Acr in the *GFP*-disruption assay. SpCas9-NLS RNP (20 pmol) targeting *GFP* was delivered via nucleofection into U2OS-EGFP.PEST cells. The cells were seeded, incubated at 37 °C, and treated with 6×NLS-Acr (0.13, 0.25, 0.5, 1, 2, or 4 μM) or LF_N-Acr (2.5×10^{-5}, 2.5×10^{-4}, 2.5×10^{-3}, 0.025, 0.25, or 2.5 μM) plus PA (20 nM) at 0 h. After 48 h, live cells were stained with Hoechst 33342 and imaged using high-throughput confocal microscopy. The values were normalized to Cas9 RNP (100%, not shown) and are the mean ± SD of three independent replicates. Some error bars are too small to visualize.

Downloaded from pubs.acs.org/jacsat/article-supplement/5420577/pdf/ja5c19089_si_001/ by guest on 21 November 2026

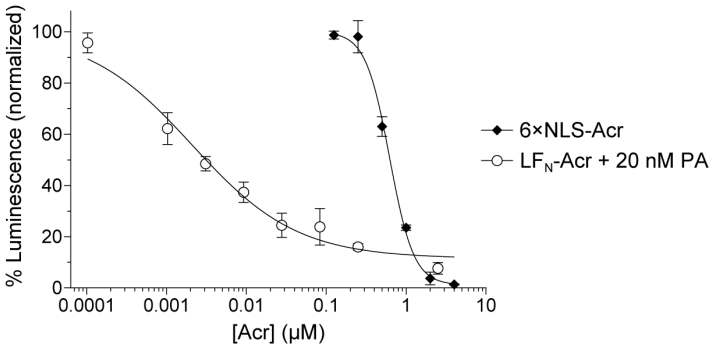


Figure S21. Dose-dependent inhibition of Cas9 by 6×NLS-Acr and LF_N-Acr in the HiBiT-knock-in assay. SpCas9-NLS RNP (20 pmol) targeting *GAPDH* and the HiBiT ssODN (80 pmol) were co-delivered via nucleofection into HUES 8 cells. The cells were seeded, incubated at 37 °C, and treated with 6×NLS-Acr (0.13, 0.25, 0.5, 1, 2, or 4 μM) or LF_N-Acr (0.0001, 0.001, 0.003, 0.009, 0.028, 0.083, 0.25, or 2.5 μM) plus PA (20 nM) at 0 h. After 24 h, the cells were lysed and combined with LgBiT and furimazine, and their luminescence was quantified. The values were normalized to Cas9 RNP with ssODN (100%, not shown) and are the mean ± SD of three independent replicates. Some error bars are too small to visualize.

Downloaded from pubs.acs.org/jacsat/article-supplement/5420577/pdf/ja5c19089_si_001/ by guest on 21 November 2026

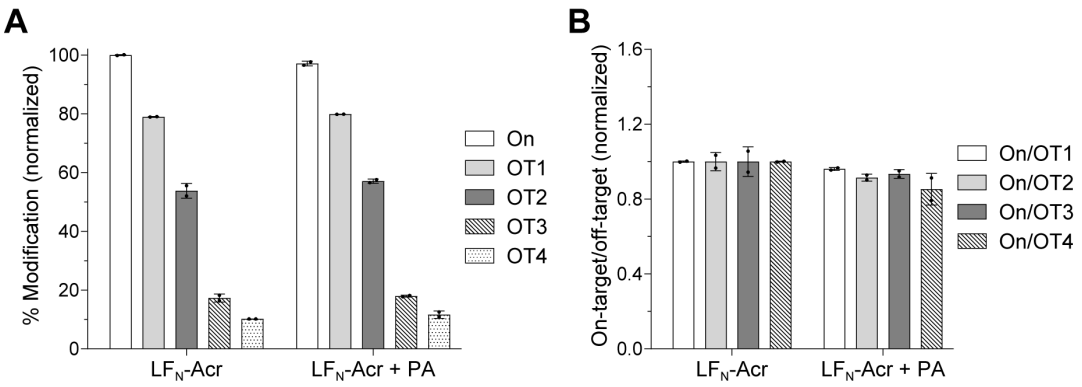


Figure S22. Effect of LF_N-Acr delivery on genome-editing activity and specificity. (A) LF_N-Acr delivery is ineffective after Cas9 lipofection. Plasmids encoding 2×NLS-SpCas9 (750 ng) and *EMX1*-targeting gRNA (250 ng) were delivered via lipofection into HEK293T cells. The cells were incubated at 37 °C and treated with LF_N-Acr (250 nM) ± PA (20 nM) at 1 h. After 72 h, genomic DNA was extracted, sequenced with NGS, and analyzed using CRISPResso2 to determine the % modification at the on-target (On) and off-target (OT1, OT2, OT3, and OT4) sites. The values were normalized to Cas9·gRNA with LF_N-Acr (On) and are the mean ± SD of two independent replicates. The significance of PA-mediated LF_N-Acr delivery was determined using an unpaired, two-tailed *t*-test versus Cas9·gRNA with LF_N-Acr (separately for On, OT1, OT2, OT3, and OT4), where *, **, ***, and **** refer to $P \leq 0.05$, $P \leq 0.01$, $P \leq 0.001$, and $P \leq 0.0001$, respectively. The differences are not statistically significant. (B) Because of its ineffective delivery after Cas9 lipofection, LF_N-Acr combined with PA does not increase Cas9 specificity. Specificity was calculated as the ratio of on-target to off-target % modification using data from panel A, normalized to the on-target to off-target % modification ratio of Cas9·gRNA with LF_N-Acr (separately for On/OT1, On/OT2, On/OT3, and On/OT4). The significance of the specificity was determined using an unpaired, two-tailed *t*-test compared to the specificity of Cas9·gRNA with LF_N-Acr (separately for On/OT1, On/OT2, On/OT3, and On/OT4), where *, **, ***, and **** refer to $P \leq 0.05$, $P \leq 0.01$, $P \leq 0.001$, and $P \leq 0.0001$, respectively. The differences are not statistically significant.

Downloaded from pubs.acs.org/jacsat/article-supplement/5420577/pdf/ja5c19089_si_001/ by guest on 21 November 2026

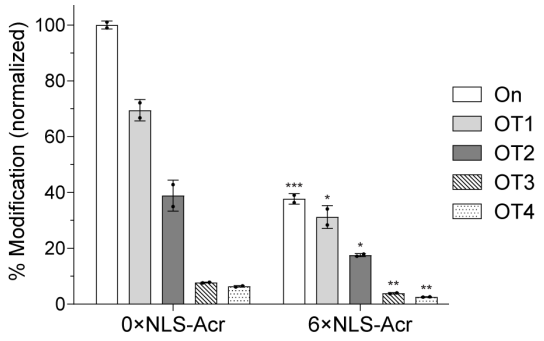


Figure S23. 6×NLS-Acr delivery regulates the activity of a less active Cas9 variant. Plasmids encoding SpCas9-NLS (750 ng) and *EMX1*-targeting gRNA (250 ng) were delivered via lipofection into HEK293T cells. The cells were incubated at 37 °C and treated with 0×NLS-Acr (4 μM, control) or 6×NLS-Acr (4 μM) at 1 h. After 72 h, genomic DNA was extracted, sequenced with NGS, and analyzed using CRISPResso2 to determine the % modification at the on-target (On) and off-target (OT1, OT2, OT3, and OT4) sites. The values were normalized to Cas9·gRNA with 0×NLS-Acr (On) and are the mean ± SD of two independent replicates. The significance of 6×NLS-Acr delivery was determined using an unpaired, two-tailed *t*-test versus Cas9·gRNA with 0×NLS-Acr (separately for On, OT1, OT2, OT3, and OT4), where *, **, ***, and **** refer to $P \leq 0.05$, $P \leq 0.01$, $P \leq 0.001$, and $P \leq 0.0001$, respectively.

Downloaded from pubs.acs.org/jacsat/article-supplement/5420577/pdf/ja5c19089_si_001/ by guest on 21 November 2026

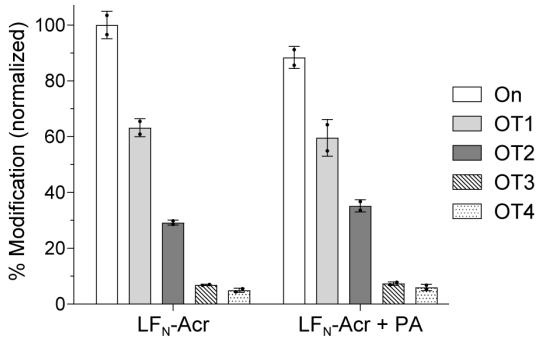


Figure S24. LF$_N$-Acr delivery is ineffective after lipofection of a less active Cas9 variant. Plasmids encoding SpCas9-NLS (750 ng) and *EMX1*-targeting gRNA (250 ng) were delivered via lipofection into HEK293T cells. The cells were incubated at 37 °C and treated with LF$_N$-Acr (250 nM) ± PA (20 nM) at 1 h. After 72 h, genomic DNA was extracted, sequenced with NGS, and analyzed using CRISPResso2 to determine the % modification at the on-target (On) and off-target (OT1, OT2, OT3, and OT4) sites. The values were normalized to Cas9·gRNA with LF$_N$-Acr (On) and are the mean ± SD of two independent replicates. The significance of PA-mediated LF$_N$-Acr delivery was determined using an unpaired, two-tailed *t*-test versus Cas9·gRNA with LF$_N$-Acr (separately for On, OT1, OT2, OT3, and OT4), where *, **, ***, and **** refer to $P \leq 0.05$, $P \leq 0.01$, $P \leq 0.001$, and $P \leq 0.0001$, respectively. The differences are not statistically significant.

Downloaded from pubs.acs.org/jacsat/article-supplement/5420577/pdf/ja5c19089_si_001/ by guest on 21 November 2026

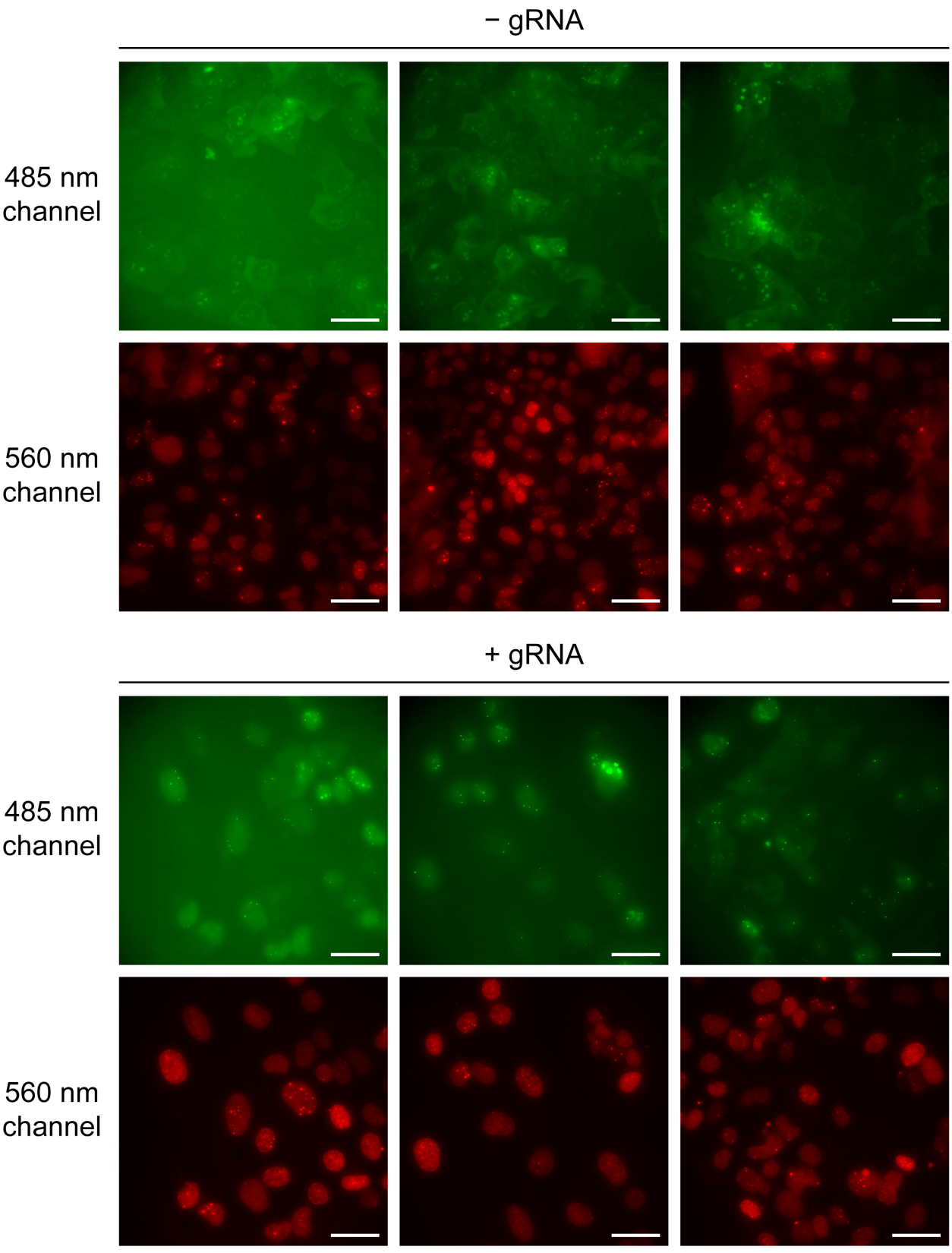


Figure S25A. (continued on the next page).

Downloaded from pubs.acs.org/jacsat/article-supplement/5420577/pdf/ja5c19089_si_001/ by guest on 21 November 2026

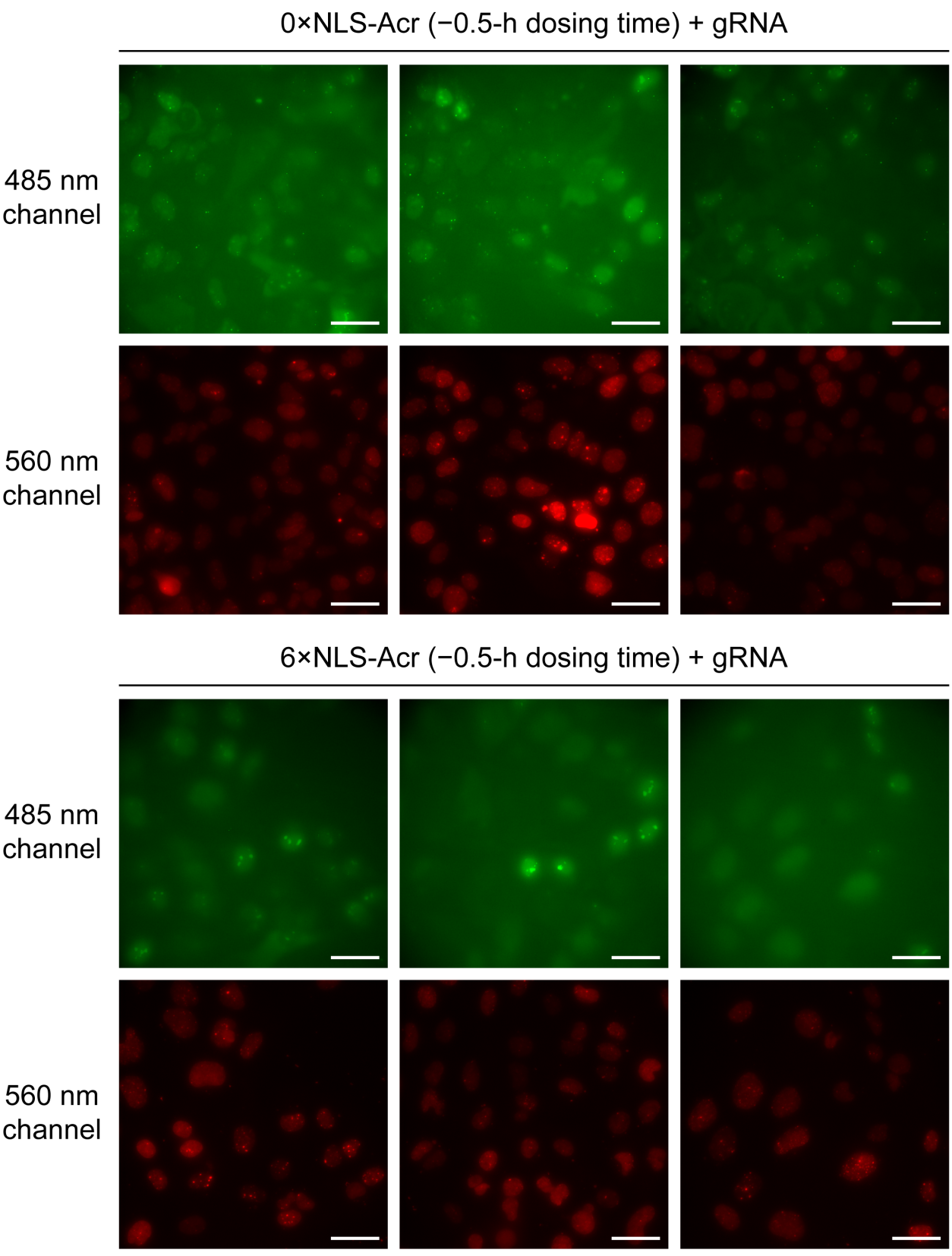


Figure S25B. (continued on the next page).

Downloaded from pubs.acs.org/jacsat/article-supplement/5420577/pdf/ja5c19089_si_001/ by guest on 21 November 2026

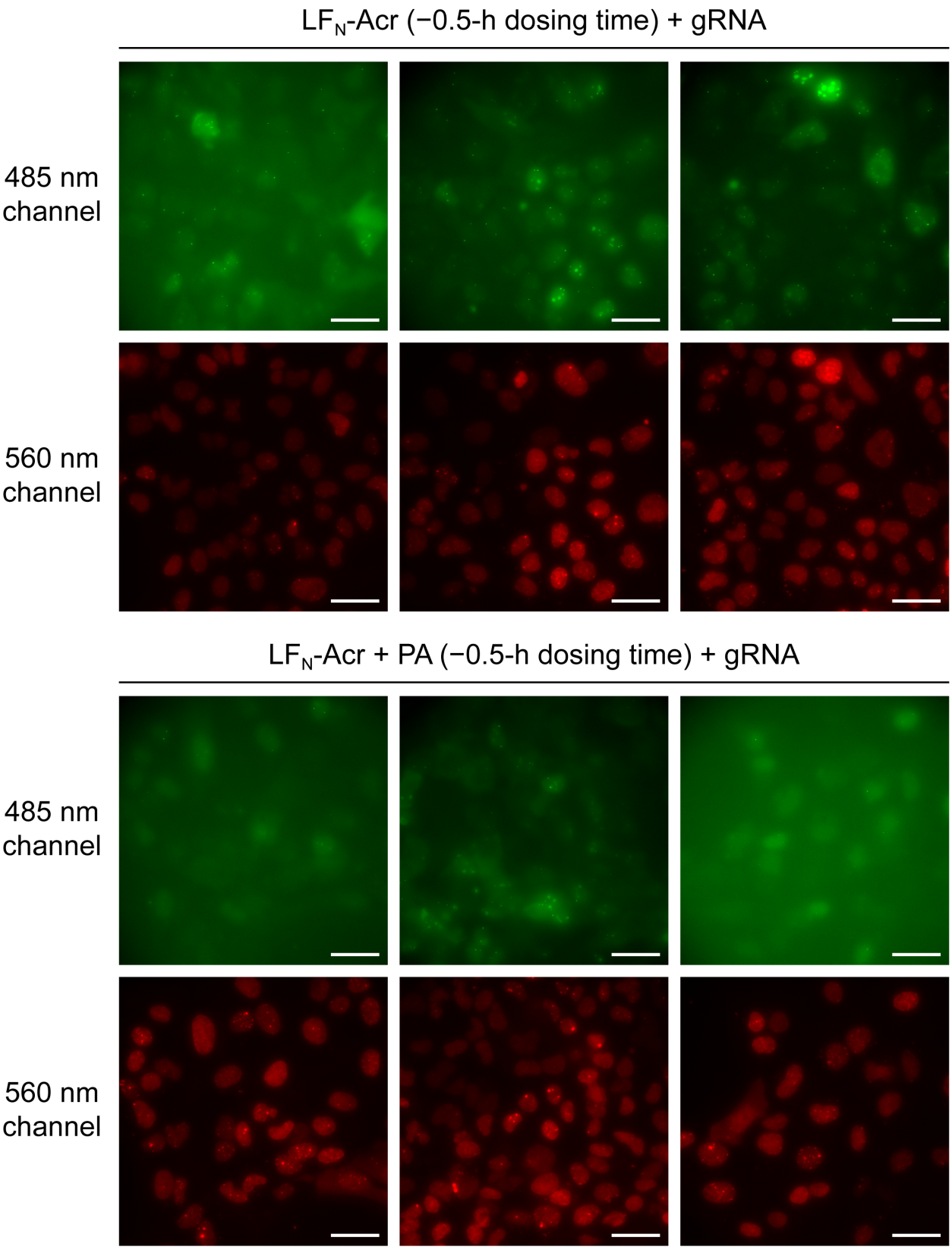


Figure S25C. (continued on the next page).

Downloaded from pubs.acs.org/jacsat/article-supplement/5420577/pdf/ja5c19089_si_001/ by guest on 21 November 2026

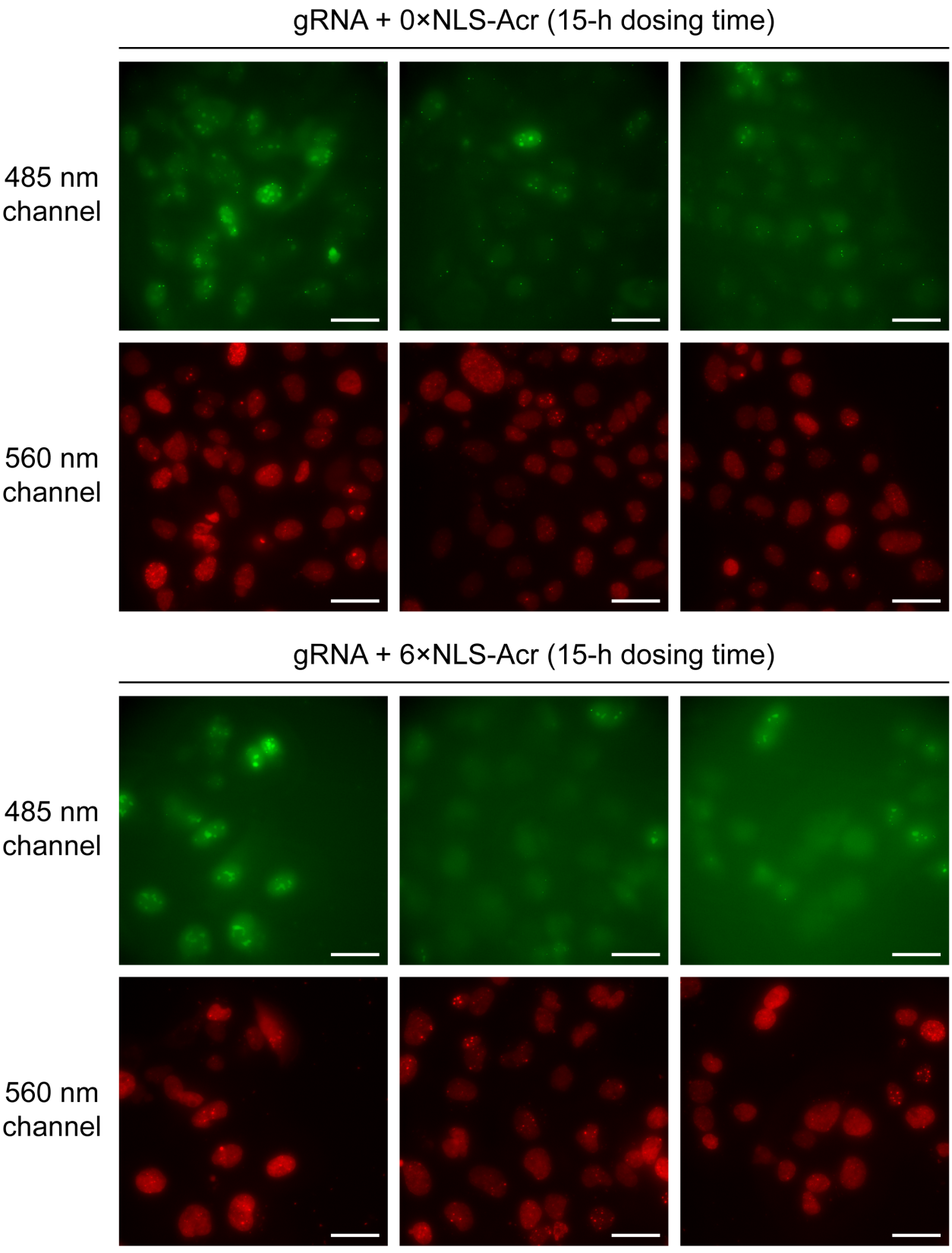


Figure S25D. (continued on the next page).

Downloaded from pubs.acs.org/jacsat/article-supplement/5420577/pdf/ja5c19089_si_001/ by guest on 21 November 2026

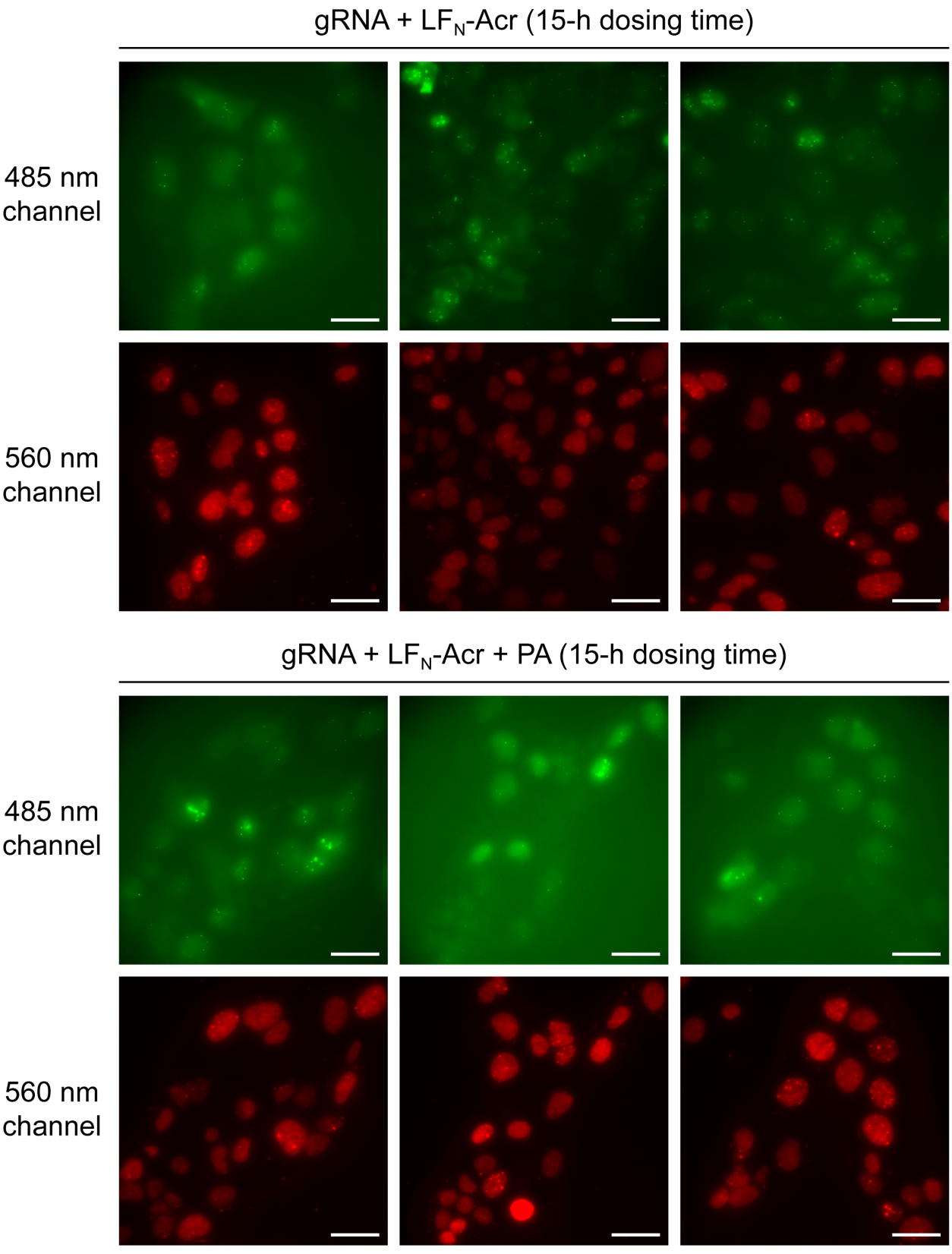


Figure S25E. (continued on the next page).

Downloaded from pubs.acs.org/jacsat/article-supplement/5420577/pdf/ja5c19089_si_001/ by guest on 21 November 2026

Figure S25. Uncropped and unmarked maximum intensity projections from the experiment described in Figure 5. (A–E) Direct visualization of the inhibition of Cas9–GFP by 6×NLS-Acr and LF_N-Acr. Ch3Rep gRNA was delivered via lipofection into a U2OS cell line stably expressing SpCas9–GFP and 53BP1–mCherry. Cells were treated with 6×NLS-Acr (2.5 μM) or LF_N-Acr (2.5 μM) plus PA (20 nM) either 0.5 h before (−0.5 h, panels B and C) or 15 h after (15 h, panels D and E) gRNA transfection. Controls include cells transfected with or without gRNA (panel A) and cells treated with 0×NLS-Acr (2.5 μM) or LF_N-Acr (2.5 μM) at −0.5 h (panels B and C) or 15 h (panels D and E). Live cells were imaged using widefield fluorescence microscopy (60× objective) at 15 h (panels A, B, and C) and 20 h (panels D and E) to detect fluorescence from Cas9–GFP (green; 485 nm excitation) and 53BP1–mCherry (red nuclear marker; 560 nm excitation). Three representative images are included for each condition. Scale bars, 40 μm.

Downloaded from pubs.acs.org/jacsat/article-supplement/5420577/pdf/ja5c19089_si_001/ by guest on 21 November 2026

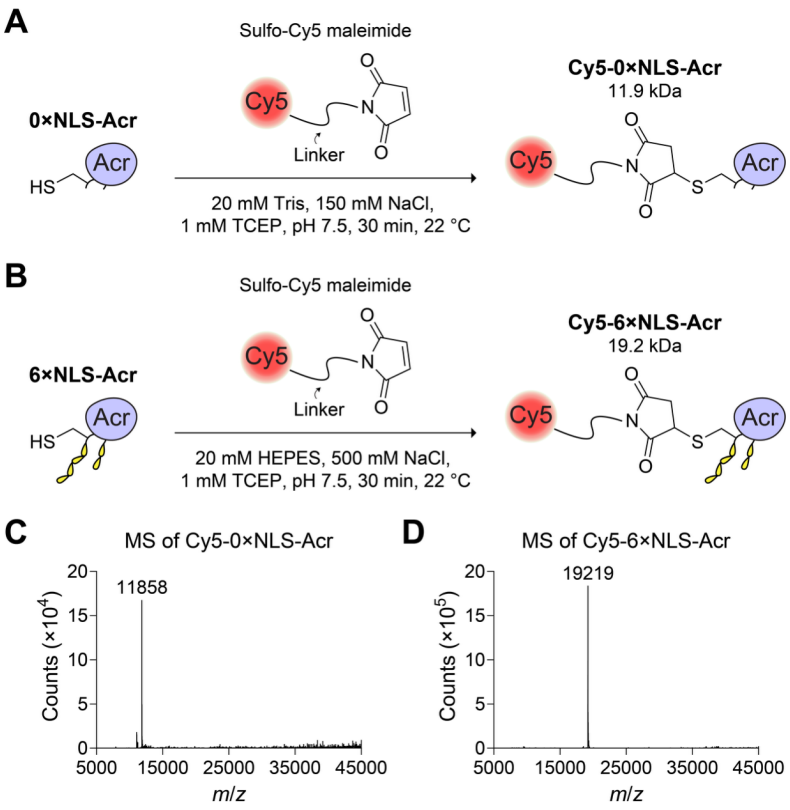


Figure S26. Synthesis and characterization of fluorescently labeled Acrs. (A) Synthesis of Cy5-0×NLS-Acr. 0×NLS-Acr was reacted with sulfo-Cy5 maleimide to generate Cy5-0×NLS-Acr. (B) Synthesis of Cy5-6×NLS-Acr. 6×NLS-Acr was reacted with sulfo-Cy5 maleimide to generate Cy5-6×NLS-Acr. (C) Q-TOF LC–MS of Cy5-0×NLS-Acr. LC–MS confirmed that 0×NLS-Acr (11,093 Da) was almost entirely converted to Cy5-0×NLS-Acr (11,858 Da). A low-abundance peak with an *m*/*z* of 11,095 was also detected in the mass spectrum. This *m*/*z* value is close to the mass of 0×NLS-Acr (11,093 Da), suggesting a small amount of unreacted 0×NLS-Acr is present. (D) Q-TOF LC–MS of Cy5-6×NLS-Acr. LC–MS confirmed that 6×NLS-Acr (18,454 Da) was fully converted to Cy5-6×NLS-Acr (19,219 Da).

Downloaded from pubs.acs.org/jacsat/article-supplement/5420577/pdf/ja5c19089_si_001/ by guest on 21 November 2026

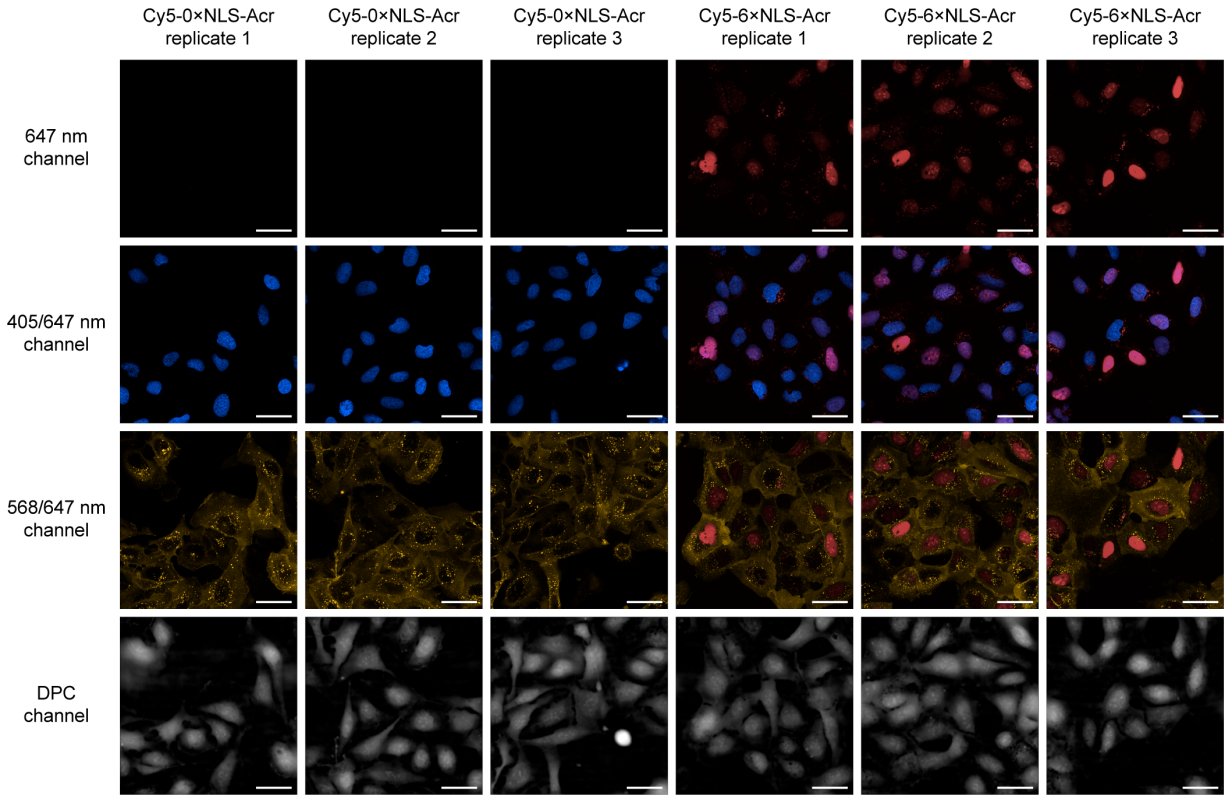


Figure S27. Visualizing the delivery of fluorescently labeled Acrs at 37 °C. U2OS cells were seeded and incubated overnight at 37 °C. Cells were then treated with Cy5-0×NLS-Acr (1.5 μM, control) or Cy5-6×NLS-Acr (1.5 μM) and incubated for 20 min at 37 °C. Cells were washed and stained with Hoechst 33342 and WGA555 in FluoroBrite DMEM, then imaged using confocal microscopy (60× objective) to detect fluorescence from Hoechst 33342 (blue nuclear marker; 405 nm excitation), WGA555 (yellow cell membrane marker; 568 nm excitation), and Cy5 (red; 647 nm excitation). Digital phase contrast (DPC) microscopy was also performed. Scale bars, 40 μm.

Downloaded from pubs.acs.org/jacsat/article-supplement/5420577/pdf/ja5c19089_si_001/ by guest on 21 November 2026

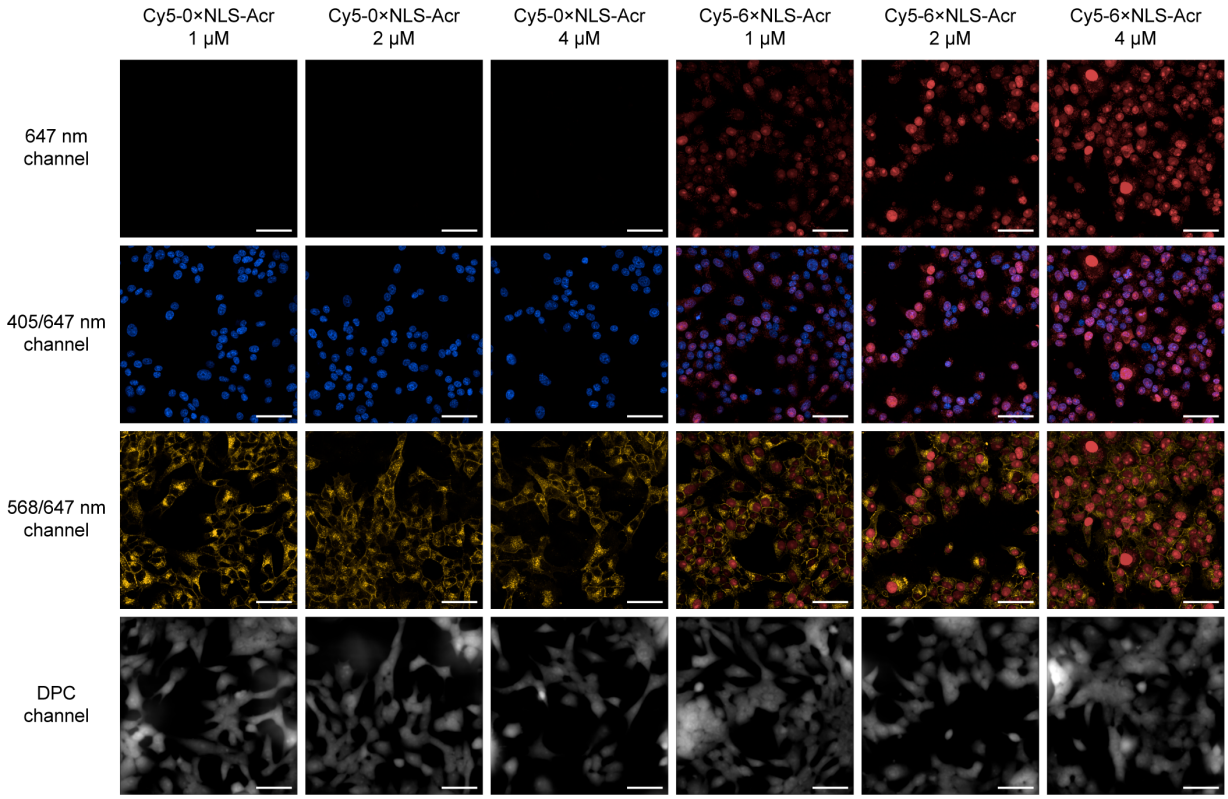


Figure S28. Dose-dependent delivery of fluorescently labeled Acrs. INS-1E rat β-cells were seeded and incubated overnight at 37 °C. Cells were then treated with Cy5-0×NLS-Acr (1–4 μM, control) or Cy5-6×NLS-Acr (1–4 μM) and incubated for 2 h at 37 °C. Cells were washed and stained with Hoechst 33342 and WGA555 in FluoroBrite DMEM, then imaged using confocal microscopy (60× objective) to detect fluorescence from Hoechst 33342 (blue nuclear marker; 405 nm excitation), WGA555 (yellow cell membrane marker; 568 nm excitation), and Cy5 (red; 647 nm excitation). Digital phase contrast (DPC) microscopy was also performed. Scale bars, 40 μm.

Downloaded from pubs.acs.org/jacsat/article-supplement/5420577/pdf/ja5c19089_si_001/ by guest on 21 November 2026

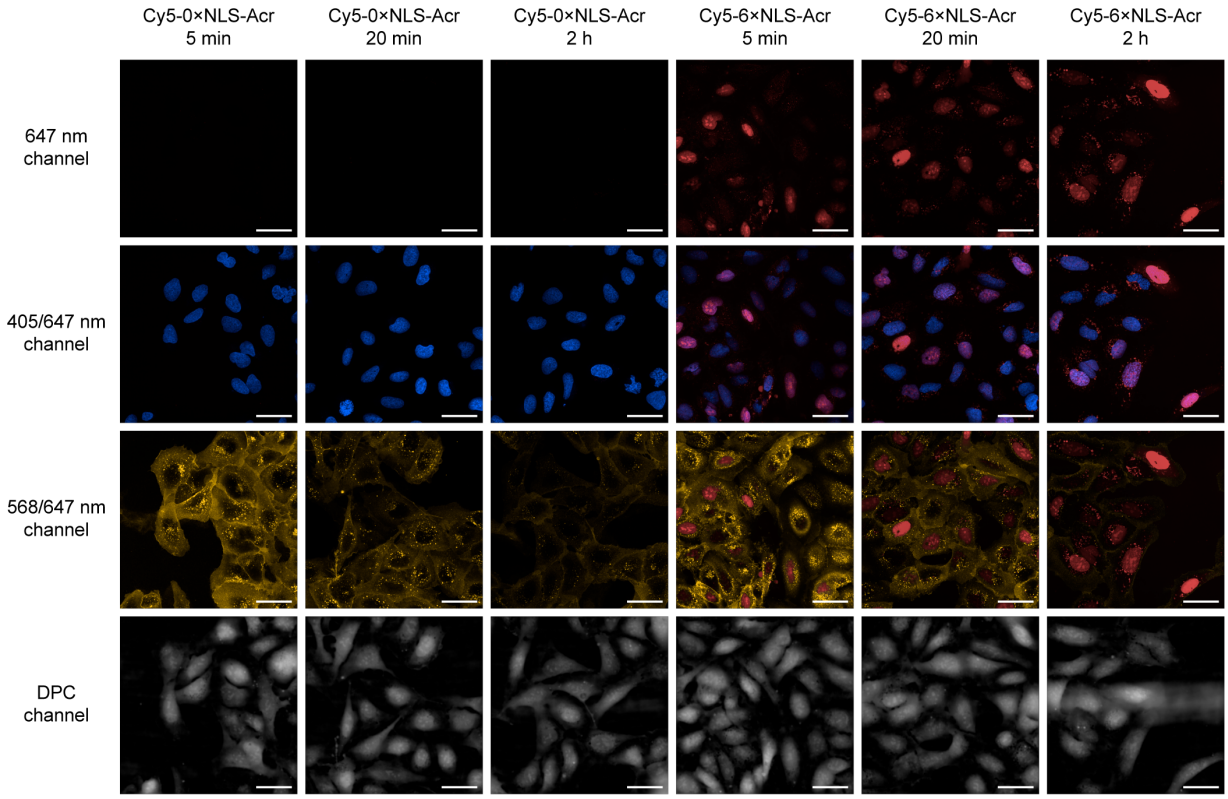


Figure S29. Time-dependent delivery of fluorescently labeled Acrs. U2OS cells were seeded and incubated overnight at 37 °C. Cells were then treated with Cy5-0×NLS-Acr (1.5 μM, control) or Cy5-6×NLS-Acr (1.5 μM) and incubated for 5 min to 2 h at 37 °C. Cells were washed and stained with Hoechst 33342 and WGA555 in FluoroBrite DMEM, then imaged using confocal microscopy (60× objective) to detect fluorescence from Hoechst 33342 (blue nuclear marker; 405 nm excitation), WGA555 (yellow cell membrane marker; 568 nm excitation), and Cy5 (red; 647 nm excitation). Digital phase contrast (DPC) microscopy was also performed. Scale bars, 40 μm.

Downloaded from pubs.acs.org/jacsat/article-supplement/5420577/pdf/ja5c19089_si_001/ by guest on 21 November 2026

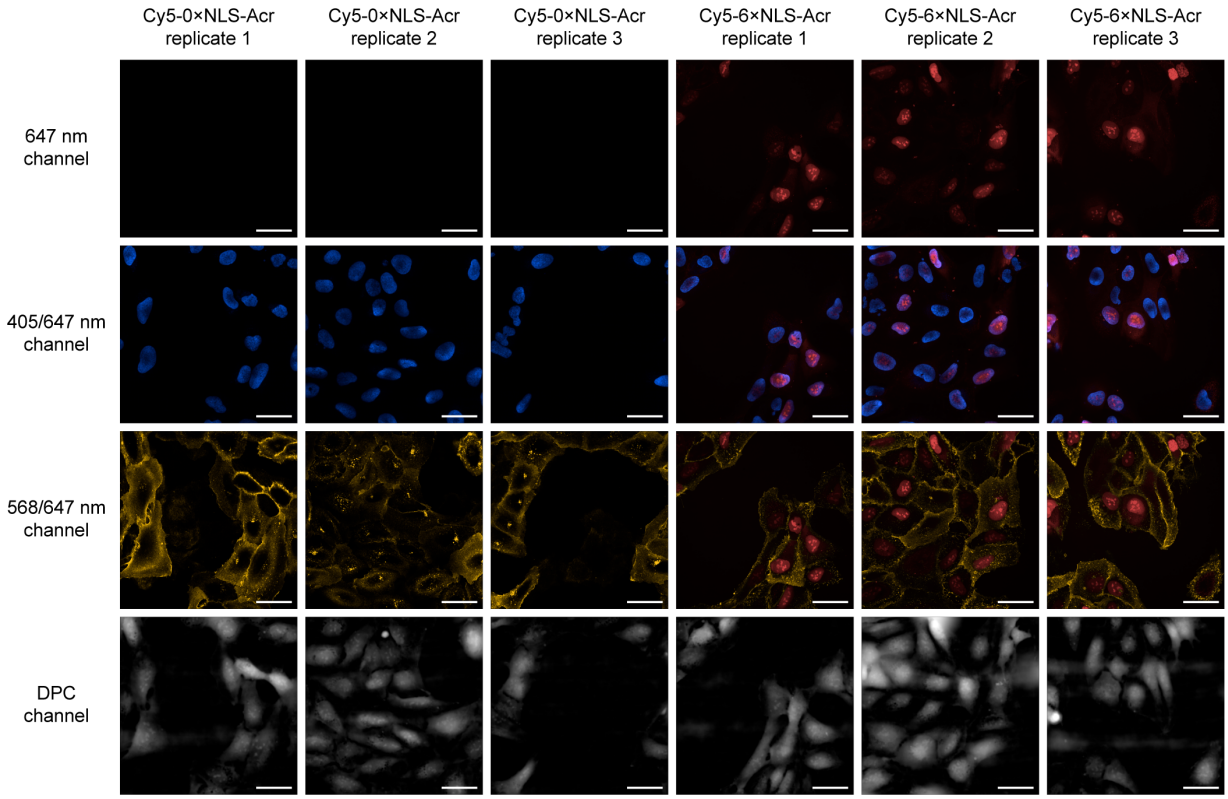


Figure S30. Visualizing the delivery of fluorescently labeled Acrs at 4 °C. U2OS cells were seeded and incubated overnight at 37 °C. Cells were then treated with Cy5-0×NLS-Acr (1.5 μM, control) or Cy5-6×NLS-Acr (1.5 μM) and incubated for 20 min at 4 °C. Cells were washed and stained with Hoechst 33342 and WGA555 in FluoroBrite DMEM, then imaged using confocal microscopy (60× objective) to detect fluorescence from Hoechst 33342 (blue nuclear marker; 405 nm excitation), WGA555 (yellow cell membrane marker; 568 nm excitation), and Cy5 (red; 647 nm excitation). Digital phase contrast (DPC) microscopy was also performed. Scale bars, 40 μm.

Downloaded from pubs.acs.org/jacsat/article-supplement/5420577/pdf/ja5c19089_si_001/ by guest on 21 November 2026

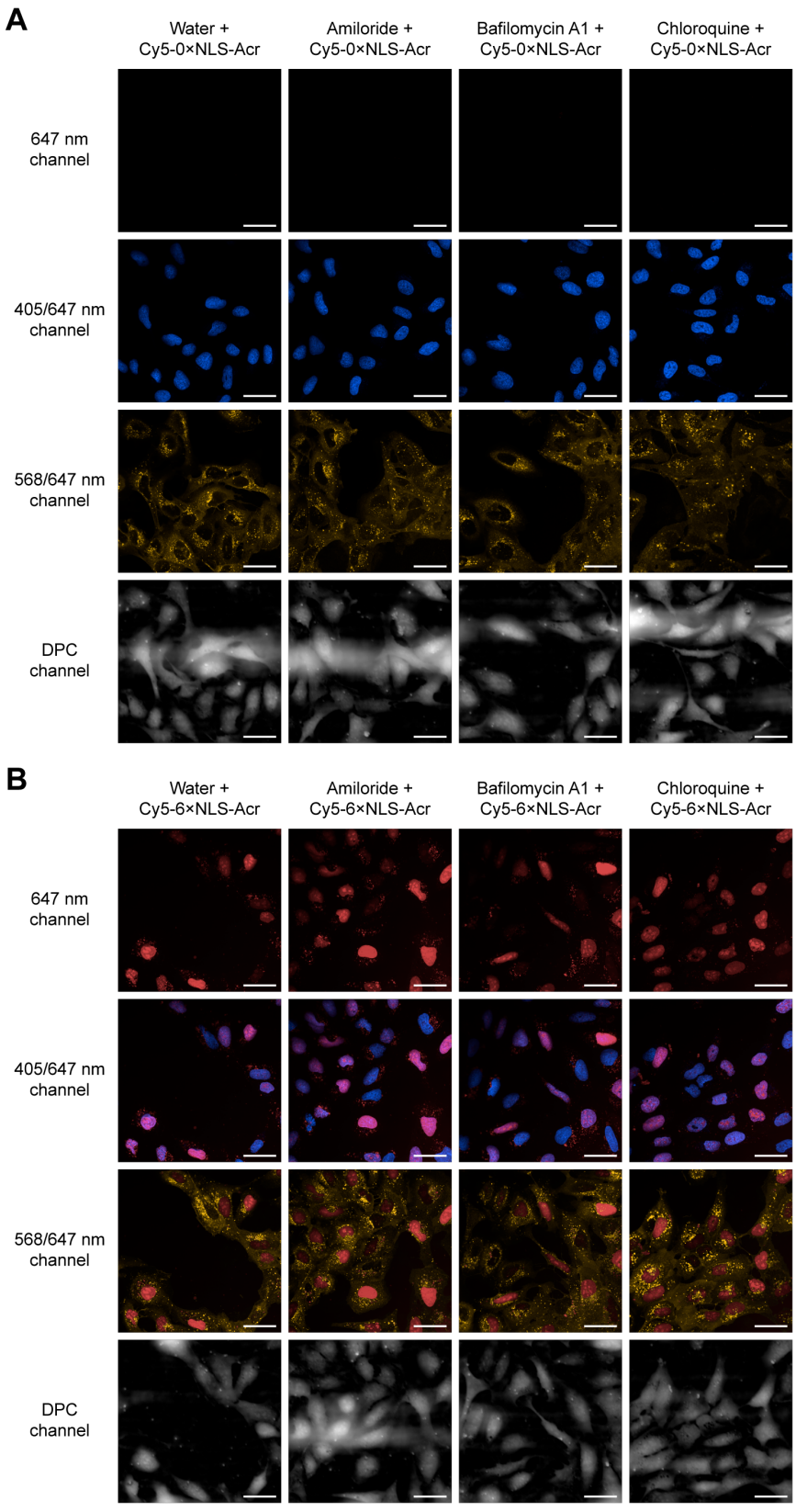


Figure S31. (continued on the next page).

Downloaded from pubs.acs.org/jacsat/article-supplement/5420577/pdf/ja5c19089_si_001/ by guest on 21 November 2026

Figure S31. Effect of small-molecule inhibitors of endocytosis on the delivery of fluorescently labeled Acrs. U2OS cells were seeded and incubated overnight at 37 °C. Cells were first treated with water (2% v/v, control) or aqueous solutions (2% v/v) of amiloride hydrochloride (50 μM), bafilomycin A1 (25 nM), or chloroquine diphosphate (100 μM), and incubated for 3 h at 37 °C. Cells were then treated with Cy5-0×NLS-Acr (1.5 μM, panel A) or Cy5-6×NLS-Acr (1.5 μM, panel B) and incubated for 20 min at 37 °C. Cells were washed and stained with Hoechst 33342 and WGA555 in FluoroBrite DMEM, then imaged using confocal microscopy (60× objective) to detect fluorescence from Hoechst 33342 (blue nuclear marker; 405 nm excitation), WGA555 (yellow cell membrane marker; 568 nm excitation), and Cy5 (red; 647 nm excitation). Digital phase contrast (DPC) microscopy was also performed. Scale bars, 40 μm.

Downloaded from pubs.acs.org/jacsat/article-supplement/5420577/pdf/ja5c19089_si_001/ by guest on 21 November 2026

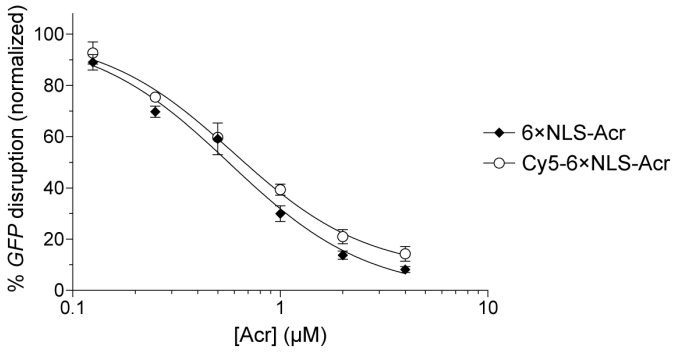


Figure S32. Dose-dependent inhibition of Cas9 by 6×NLS-Acr and Cy5-6×NLS-Acr in the *GFP*-disruption assay. SpCas9-NLS RNP (20 pmol) targeting *GFP* was delivered via nucleofection into U2OS-EGFP.PEST cells. The cells were seeded at a density of 20,000 cells per well in 100 µL of culture medium, incubated at 37 °C, and treated with 6×NLS-Acr or Cy5-6×NLS-Acr (0.13, 0.25, 0.5, 1, 2, or 4 µM) at 0 h. After 30 h, live cells were stained with Hoechst 33342 and imaged using high-throughput confocal microscopy. The values were normalized to Cas9 RNP (100%, not shown) and are the mean ± SD of three independent replicates. Some error bars are too small to visualize.

Downloaded from pubs.acs.org/jacsat/article-supplement/5420577/pdf/ja5c19089_si_001/ by guest on 21 November 2026

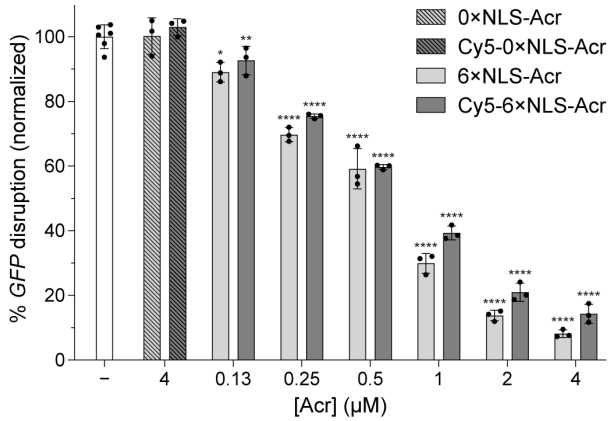


Figure S33. Dose-dependent inhibition of Cas9 by 6×NLS-Acr and Cy5-6×NLS-Acr in the *GFP*-disruption assay. SpCas9-NLS RNP (20 pmol) targeting *GFP* was delivered via nucleofection into U2OS-EGFP.PEST cells. The cells were seeded at a density of 20,000 cells per well in 100 μL of culture medium, incubated at 37 °C, and treated with 6×NLS-Acr or Cy5-6×NLS-Acr (0.13, 0.25, 0.5, 1, 2, or 4 μM) at 0 h. After 30 h, live cells were stained with Hoechst 33342 and imaged using high-throughput confocal microscopy. Controls include nucleofection of Cas9 RNP (white bar) and nucleofection of Cas9 RNP followed by treatment with 0×NLS-Acr (4 μM) or Cy5-0×NLS-Acr (4 μM) at 0 h. The values were normalized to Cas9 RNP and are the mean ± SD of three independent replicates. The significance of 6×NLS-Acr or Cy5-6×NLS-Acr delivery was determined with an unpaired, two-tailed *t*-test versus Cas9 RNP, where *, **, ***, and **** refer to $P \leq 0.05$, $P \leq 0.01$, $P \leq 0.001$, and $P \leq 0.0001$, respectively.

Downloaded from pubs.acs.org/jacsat/article-supplement/5420577/pdf/ja5c19089_si_001/ by guest on 21 November 2026

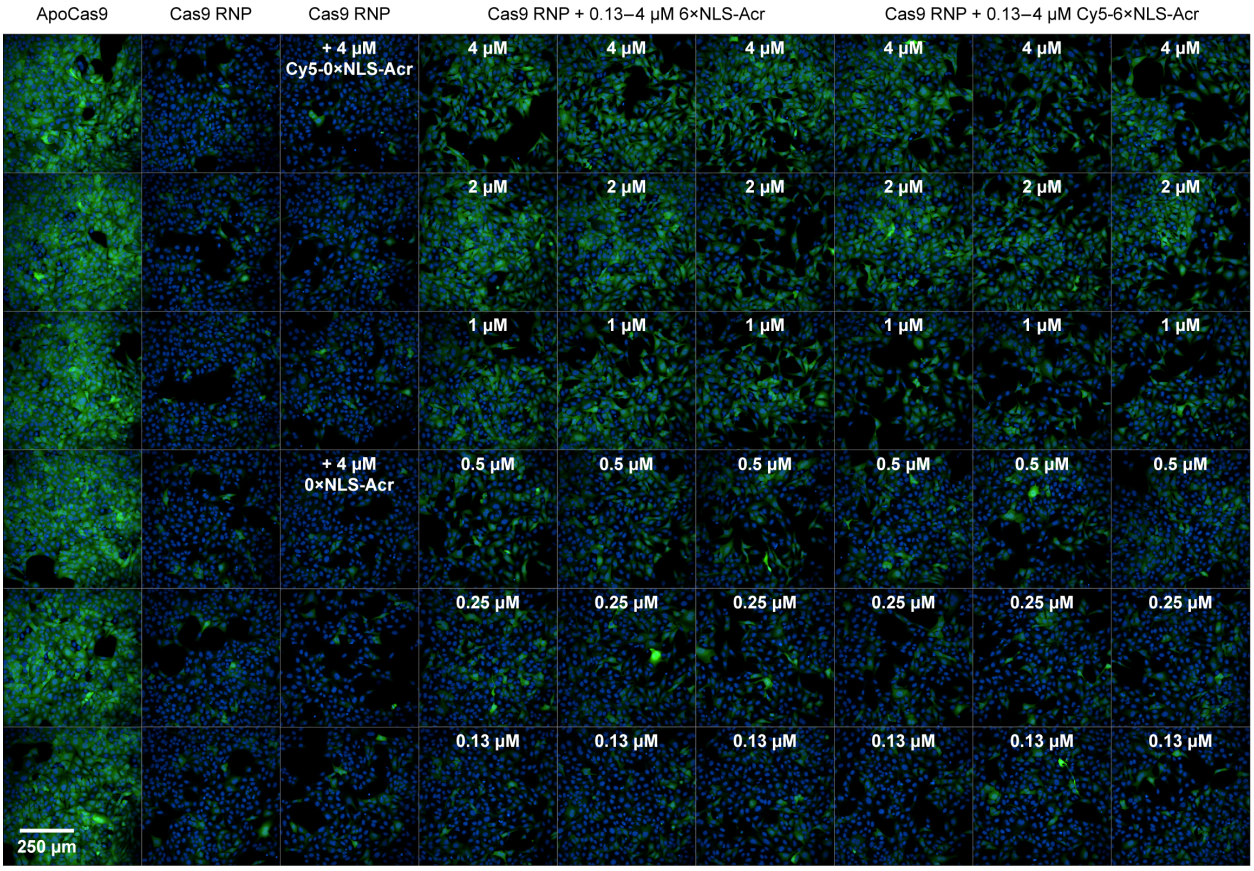


Figure S34. Representative fluorescence images from the *GFP*-disruption assay in Figure S33. SpCas9-NLS RNP (20 pmol) targeting *GFP* was delivered via nucleofection into U2OS-EGFP.PEST cells. The cells were seeded at a density of 20,000 cells per well in 100 µL of culture medium, incubated at 37 °C, and treated with 6×NLS-Acr or Cy5-6×NLS-Acr (0.13, 0.25, 0.5, 1, 2, or 4 µM) at 0 h. After 30 h, live cells were stained with Hoechst 33342 (blue, nucleus) and imaged using high-throughput confocal microscopy. Controls include nucleofection of Apo-Cas9, nucleofection of Cas9 RNP, and nucleofection of Cas9 RNP followed by treatment with 0×NLS-Acr (4 µM) or Cy5-0×NLS-Acr (4 µM) at 0 h.

Downloaded from pubs.acs.org/jacsat/article-supplement/5420577/pdf/ja5c19089_si_001/ by guest on 21 November 2026

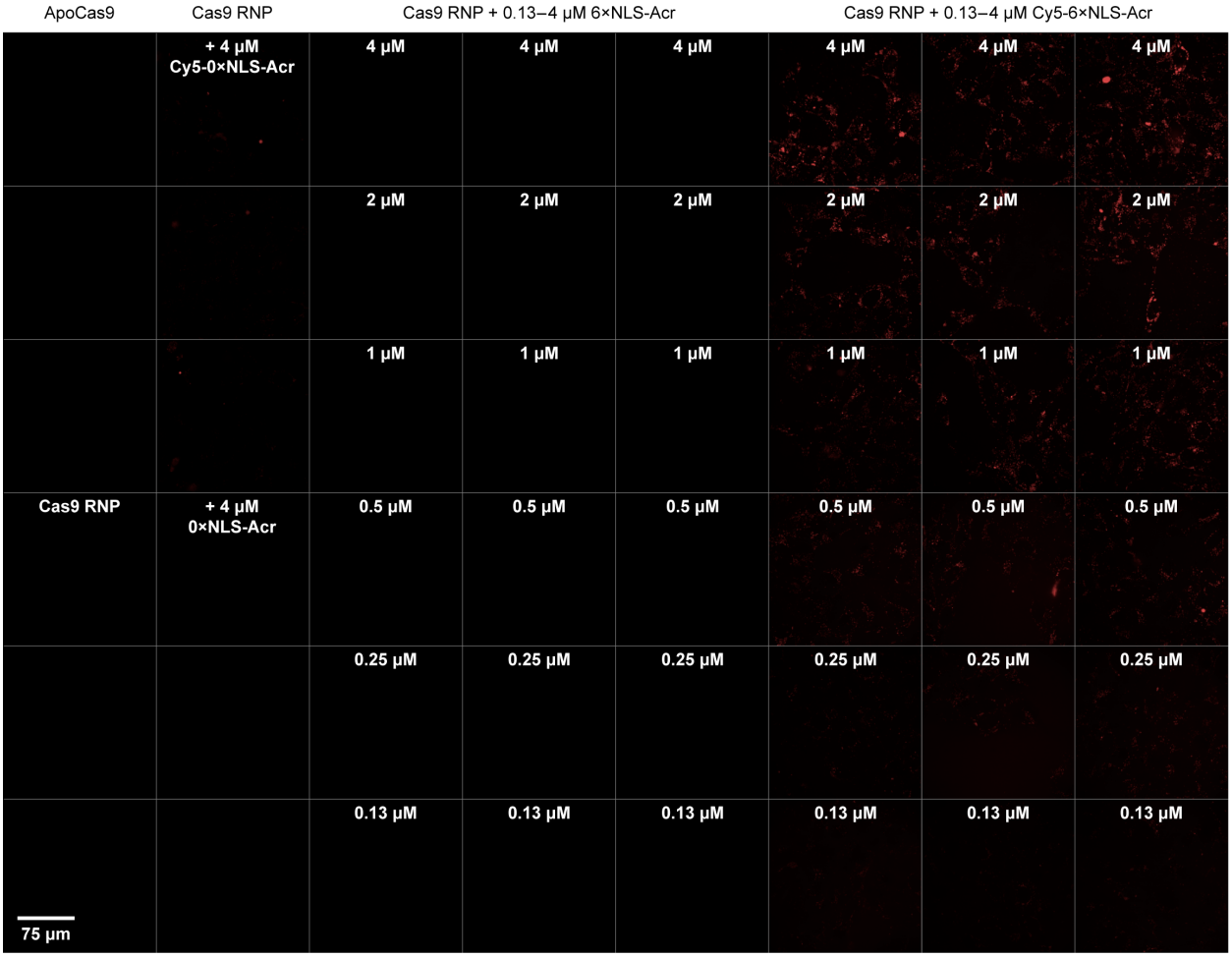


Figure S35A. 647 nm channel (continued on the next page).

Downloaded from pubs.acs.org/jacsat/article-supplement/5420577/pdf/ja5c19089_si_001/ by guest on 21 November 2026

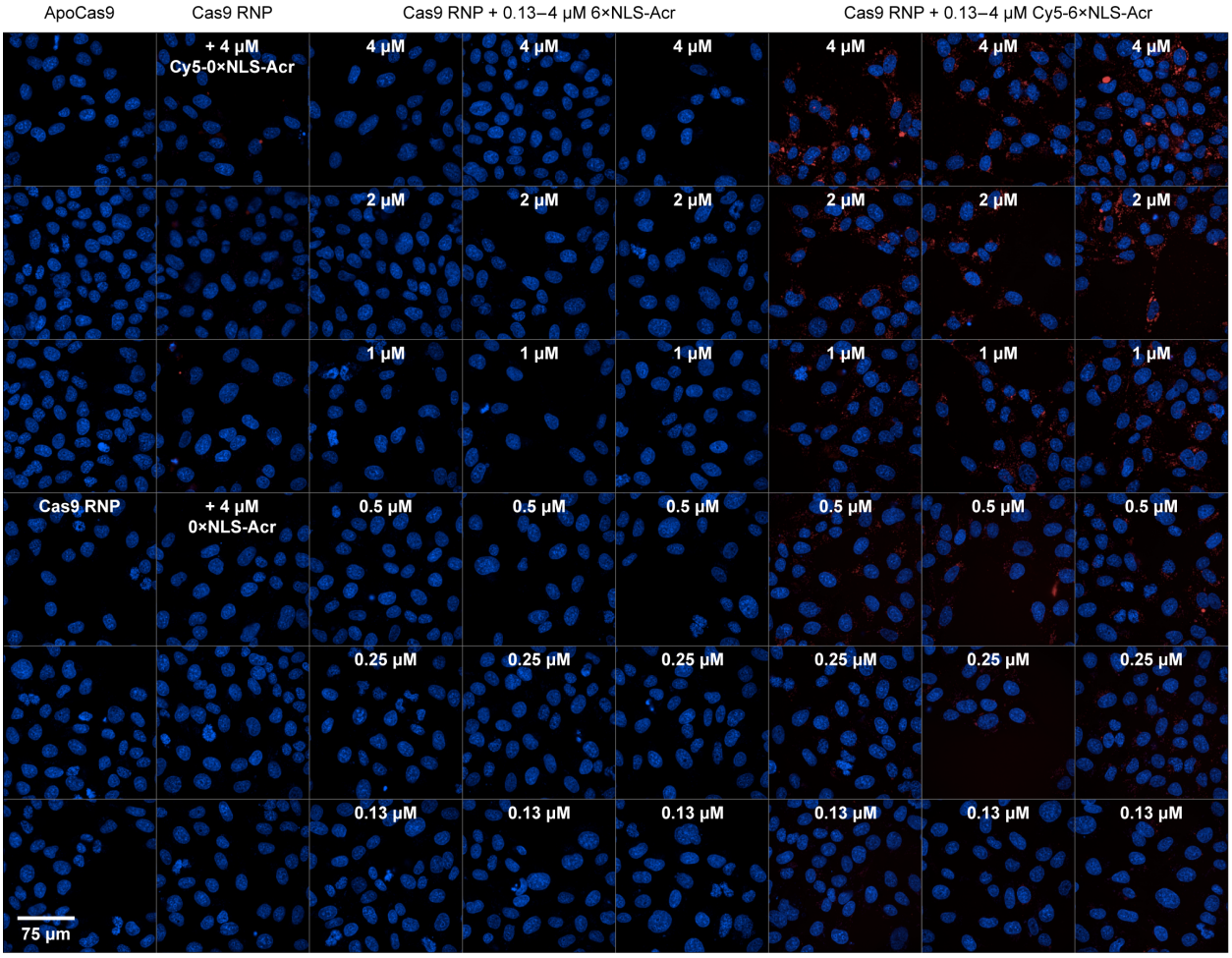


Figure S35B. 405/647 nm channel (continued on the next page).

Downloaded from pubs.acs.org/jacsat/article-supplement/5420577/pdf/ja5c19089_si_001/ by guest on 21 November 2026

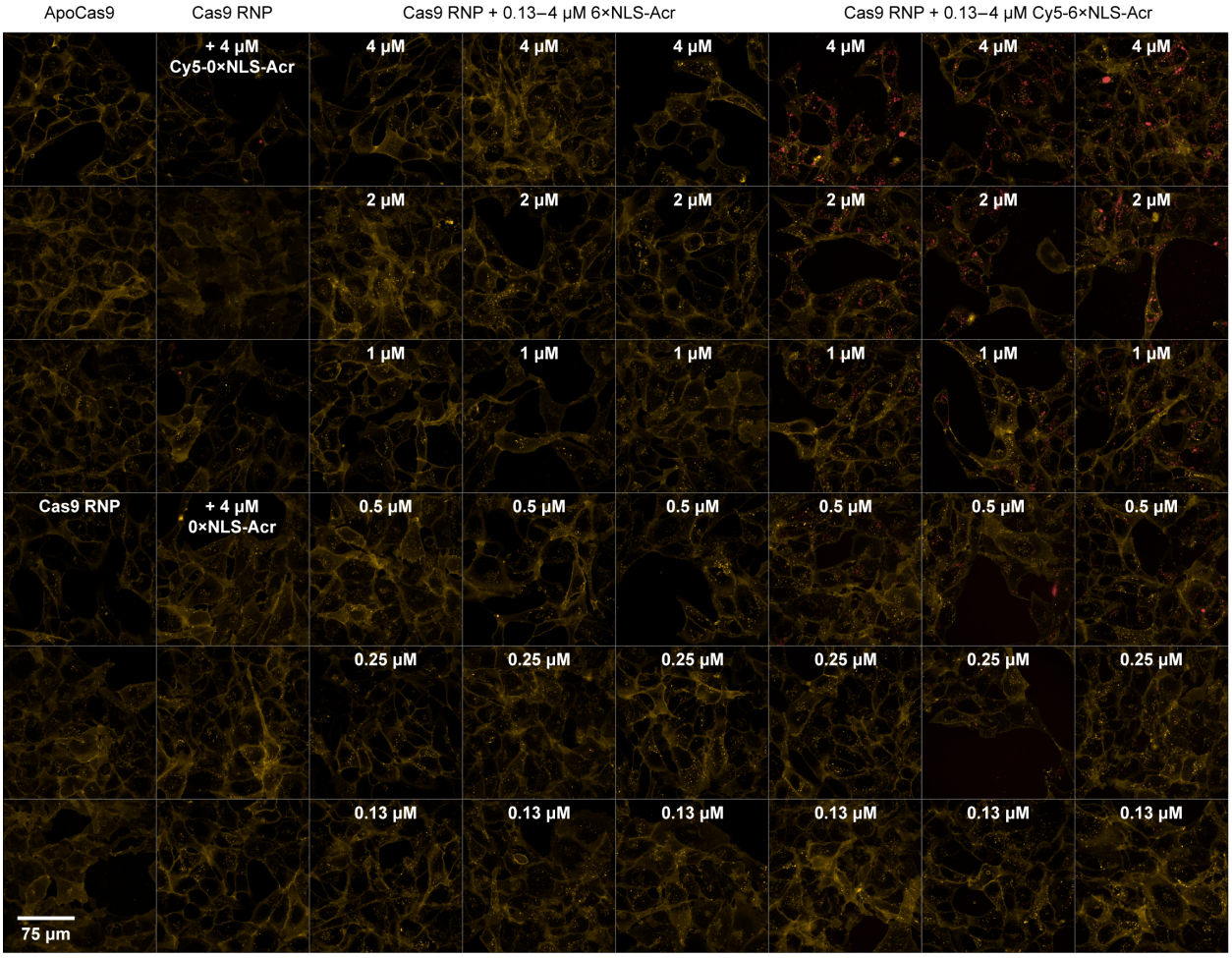


Figure S35C. 568/647 nm channel (continued on the next page).

Downloaded from pubs.acs.org/jacsat/article-supplement/5420577/pdf/ja5c19089_si_001/ by guest on 21 November 2026

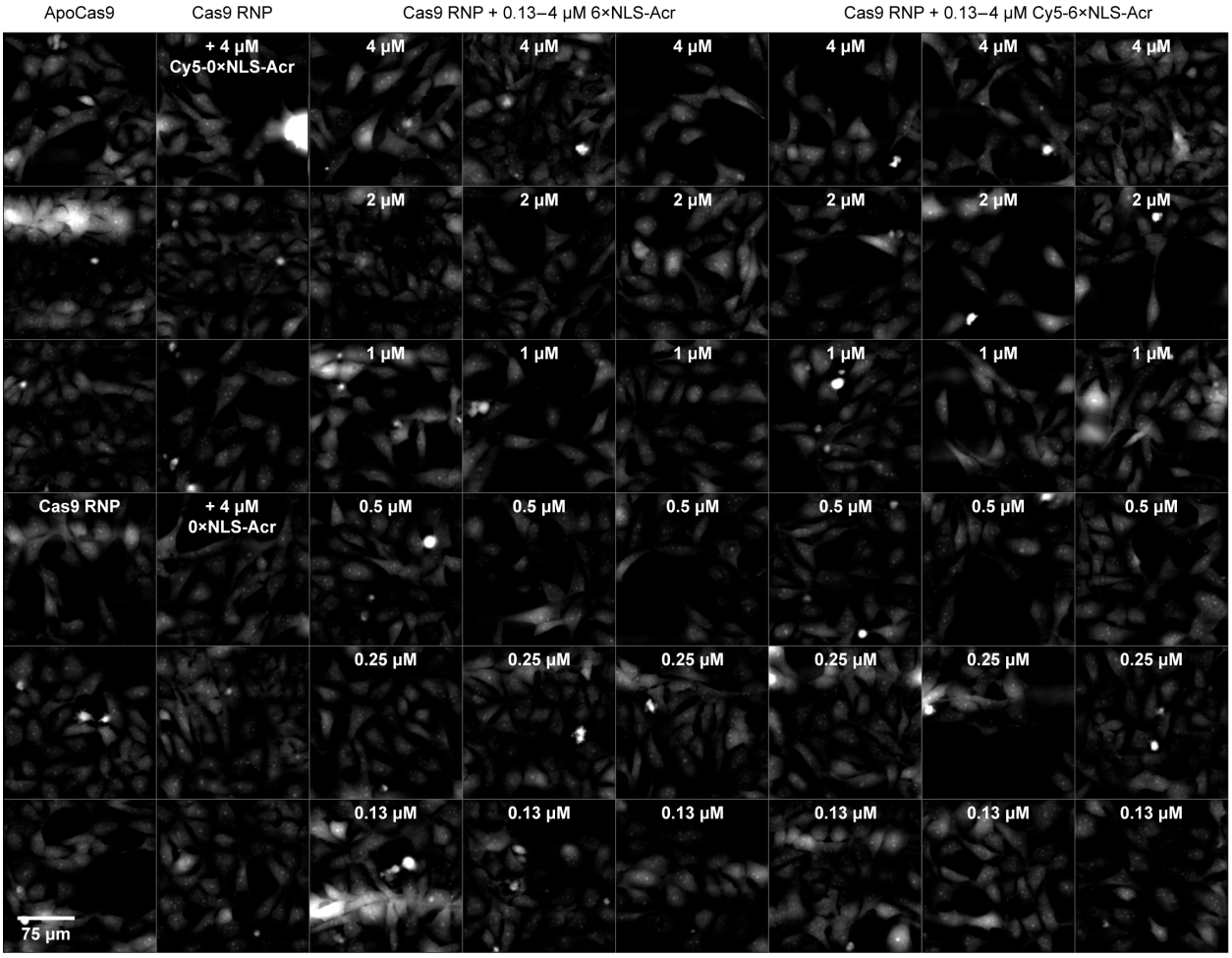


Figure S35D. DPC channel.

Figure S35. Direct visualization of Cy5-6×NLS-Acr delivery in the *GFP*-disruption assay. (A–D) SpCas9-NLS RNP (20 pmol) targeting *GFP* was delivered via nucleofection into U2OS-EGFP.PEST cells. The cells were seeded at a density of 20,000 cells per well in 100 µL of culture medium, incubated at 37 °C, and treated with 6×NLS-Acr or Cy5-6×NLS-Acr (0.13, 0.25, 0.5, 1, 2, or 4 µM) at 0 h. After 30 h, live cells were washed and stained with Hoechst 33342 and WGA555 in FluoroBrite DMEM, then imaged using high-throughput confocal microscopy (60× objective) to detect fluorescence from Hoechst 33342 (blue nuclear marker; 405 nm excitation), WGA555 (yellow cell membrane marker; 568 nm excitation), and Cy5 (red; 647 nm excitation). Digital phase contrast (DPC) microscopy was also performed. Controls include nucleofection of Apo-Cas9, nucleofection of Cas9 RNP, and nucleofection of Cas9 RNP followed by treatment with 0×NLS-Acr (4 µM) or Cy5-0×NLS-Acr (4 µM) at 0 h. These are the same wells shown in Figure S34, imaged at higher magnification, with the GFP channel omitted for clarity. Panels A, B, C, and D contain the 647 nm, 405/647 nm, 568/647 nm, and DPC channels, respectively.

Downloaded from pubs.acs.org/jacsat/article-supplement/5420577/pdf/ja5c19089_si_001/ by guest on 21 November 2026

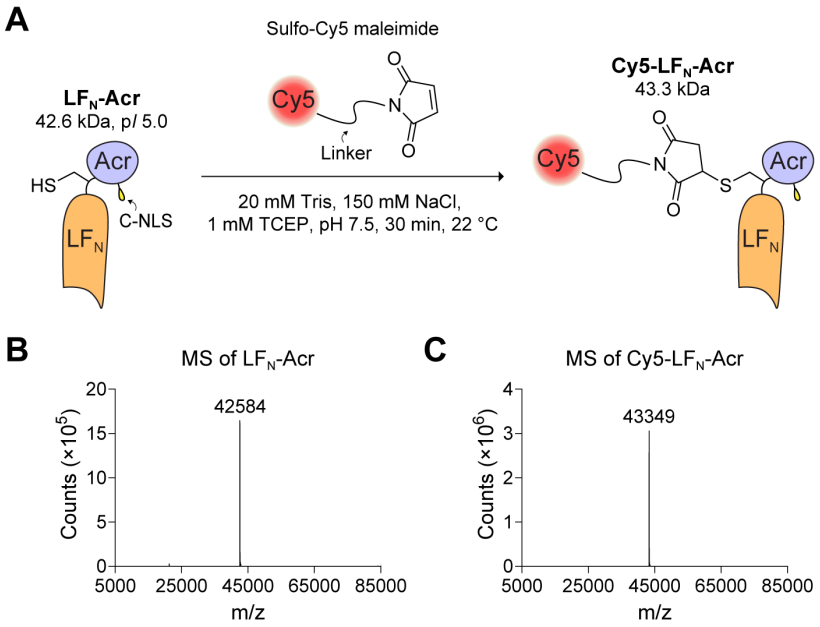


Figure S36. Synthesis and characterization of Cy5-LFN-Acr. (A) Synthesis of Cy5-LF_N-Acr. LF_N-Acr was reacted with sulfo-Cy5 maleimide to generate Cy5-LF_N-Acr. (B) Q-TOF LC–MS of LF_N-Acr. (C) Q-TOF LC–MS of Cy5-LF_N-Acr. LC–MS confirmed that LF_N-Acr (42,584 Da) was fully converted to Cy5-LF_N-Acr (43,349 Da).

Downloaded from pubs.acs.org/jacsat/article-supplement/5420577/pdf/ja5c19089_si_001/ by guest on 21 November 2026

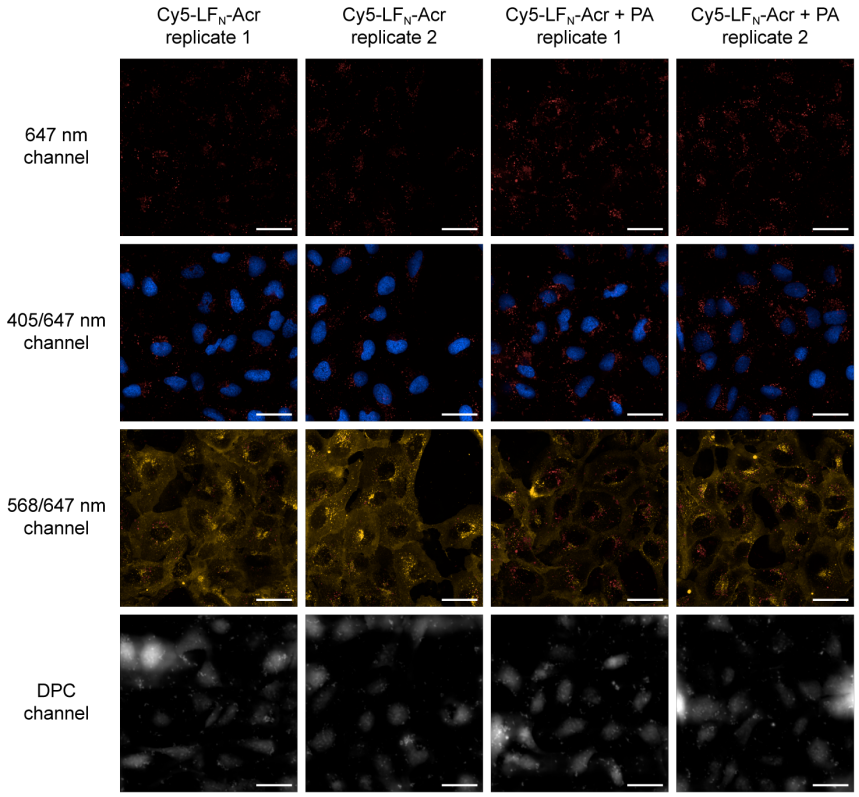


Figure S37. Visualizing the delivery of fluorescently labeled LF$_N$-Acr. U2OS cells were seeded and incubated overnight at 37 °C. Cells were then treated with LF$_N$-Acr (2.5 μM) ± PA (20 nM) and incubated for 2 h at 37 °C. Cells were washed and stained with Hoechst 33342 and WGA555 in FluoroBrite DMEM, then imaged using confocal microscopy (60× objective) to detect fluorescence from Hoechst 33342 (blue nuclear marker; 405 nm excitation), WGA555 (yellow cell membrane marker; 568 nm excitation), and Cy5 (red; 647 nm excitation). Digital phase contrast (DPC) microscopy was also performed. Scale bars, 40 μm.

Downloaded from pubs.acs.org/jacsat/article-supplement/5420577/pdf/ja5c19089_si_001/ by guest on 21 November 2026

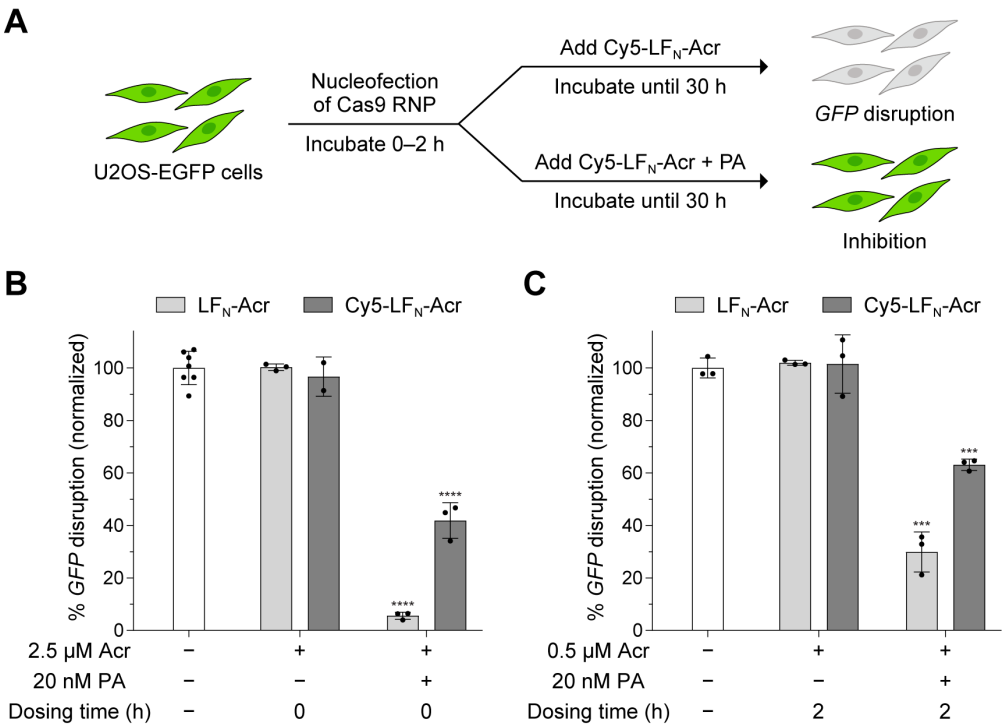


Figure S38. Effect of Cy5-LF$_N$-Acr delivery on *GFP* disruption. (A) A cartoon illustrating the experimental setup for monitoring Cy5-Acr delivery and activity in the *GFP*-disruption assay. Cy5-Acr delivery prevents *GFP* disruption. (B, C) Inhibition of Cas9 by Cy5-LF$_N$-Acr in the *GFP*-disruption assay. SpCas9-NLS RNP (20 pmol) targeting *GFP* was delivered via nucleofection into U2OS-EGFP.PEST cells. The cells were seeded at a density of 20,000 cells per well in 100 µL of culture medium, incubated at 37 °C, and treated with Cy5-LF$_N$-Acr (0.5–2.5 µM) ± PA (20 nM) at 0 h (panel B) or 2 h (panel C). After 30 h, live cells were stained with Hoechst 33342 and imaged using high-throughput confocal microscopy. Controls include nucleofection of Cas9 RNP (white bar) and nucleofection of Cas9 RNP followed by treatment with LF$_N$-Acr (0.5–2.5 µM) ± PA (20 nM) at 0 h (panel B) or 2 h (panel C). The values were normalized to Cas9 RNP and are the mean ± SD of three independent replicates. The significance of PA-mediated LF$_N$-Acr delivery was determined with an unpaired, two-tailed *t*-test versus Cas9 RNP, where *, **, ***, and **** refer to $P \leq 0.05$, $P \leq 0.01$, $P \leq 0.001$, and $P \leq 0.0001$, respectively.

Downloaded from pubs.acs.org/jacsat/article-supplement/5420577/pdf/ja5c19089_si_001/ by guest on 21 November 2026

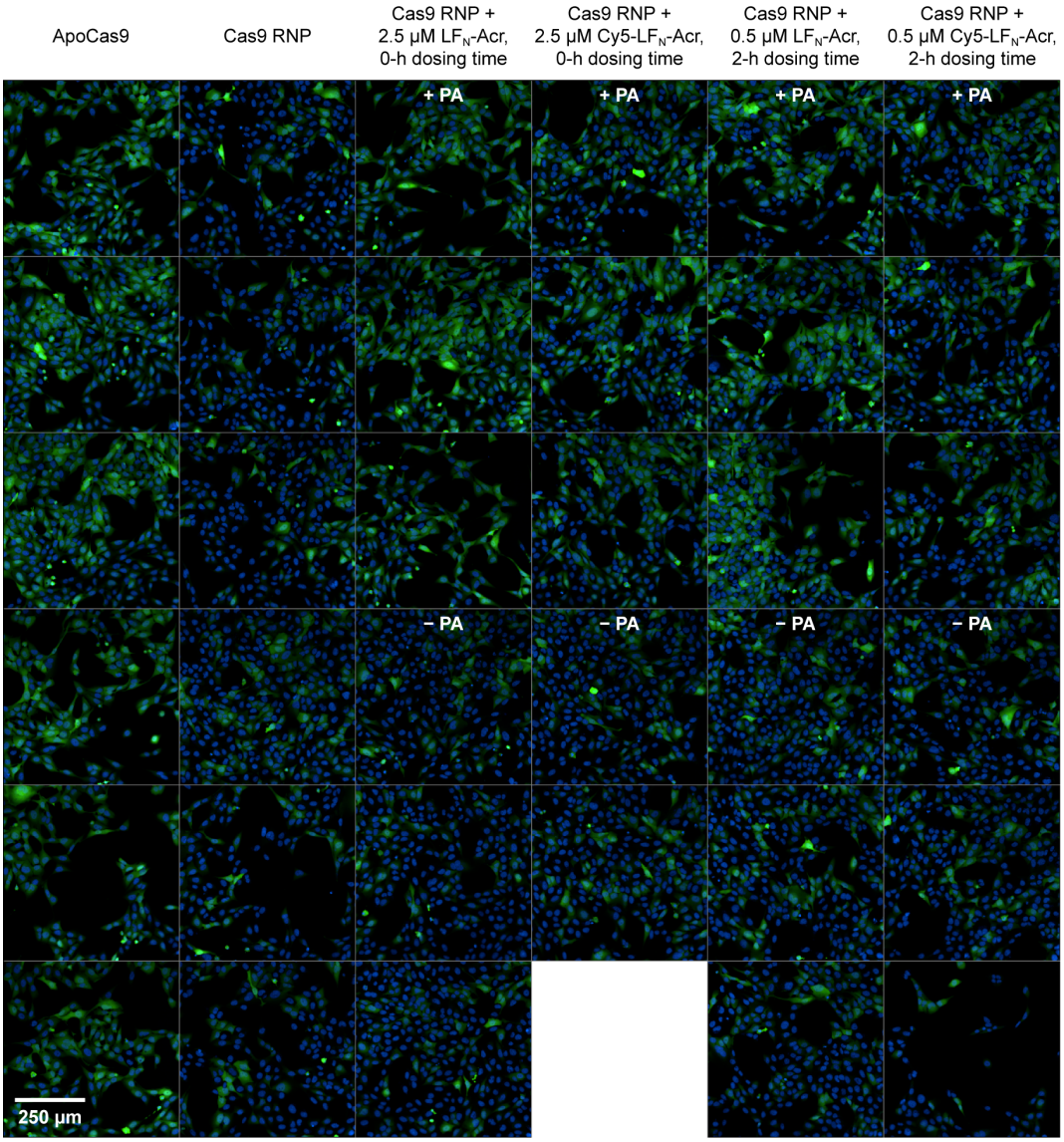


Figure S39. Representative fluorescence images from the *GFP*-disruption assay in Figure S38. SpCas9-NLS RNP (20 pmol) targeting *GFP* was delivered via nucleofection into U2OS-EGFP.PEST cells. The cells were seeded at a density of 20,000 cells per well in 100 μL of culture medium, incubated at 37 °C, and treated with Cy5-LF$_N$-Acr (0.5–2.5 μM) ± PA (20 nM) at 0 or 2 h. After 30 h, live cells were stained with Hoechst 33342 (blue, nucleus) and imaged using high-throughput confocal microscopy (20× objective). Controls include nucleofection of Cas9 RNP and nucleofection of Cas9 RNP followed by treatment with LF$_N$-Acr (0.5–2.5 μM) ± PA (20 nM) at 0 or 2 h.

Downloaded from pubs.acs.org/jacsat/article-supplement/5420577/pdf/ja5c19089_si_001/ by guest on 21 November 2026

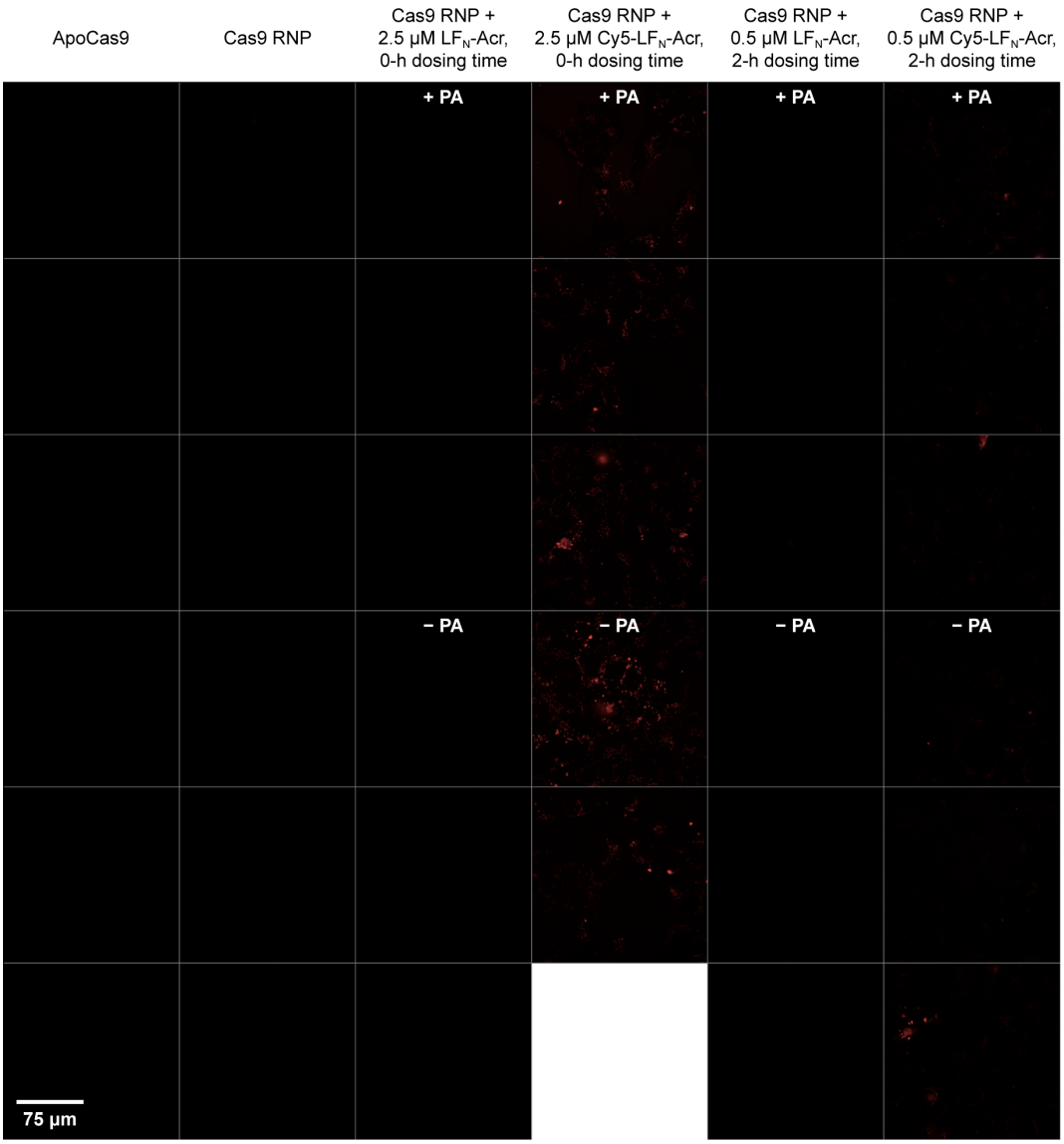


Figure S40A. 647 nm channel (continued on the next page).

Downloaded from pubs.acs.org/jacsat/article-supplement/5420577/pdf/ja5c19089_si_001/ by guest on 21 November 2026

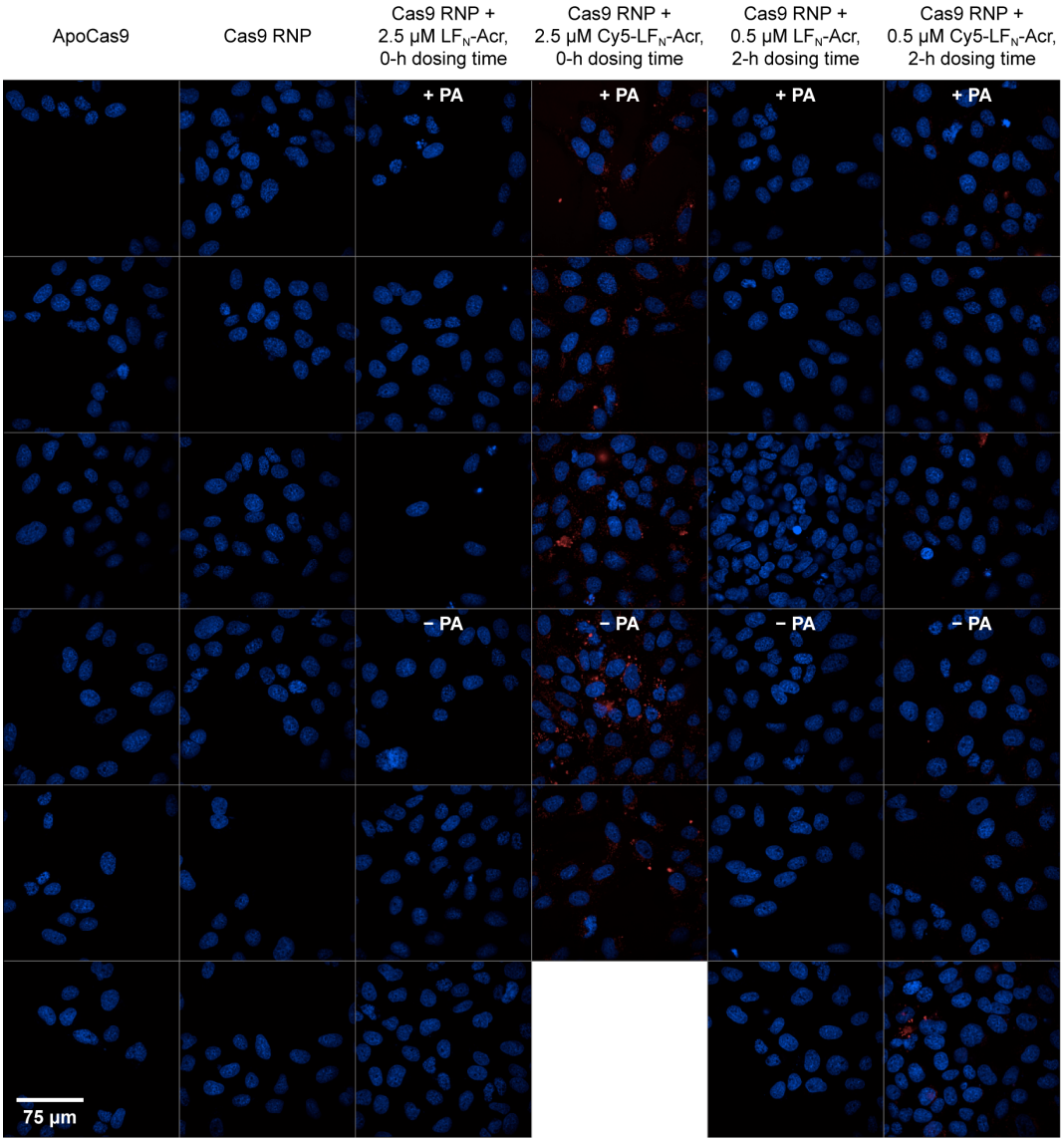


Figure S40B. 405/647 nm channel (continued on the next page).

Downloaded from pubs.acs.org/jacsat/article-supplement/5420577/pdf/ja5c19089_si_001/ by guest on 21 November 2026

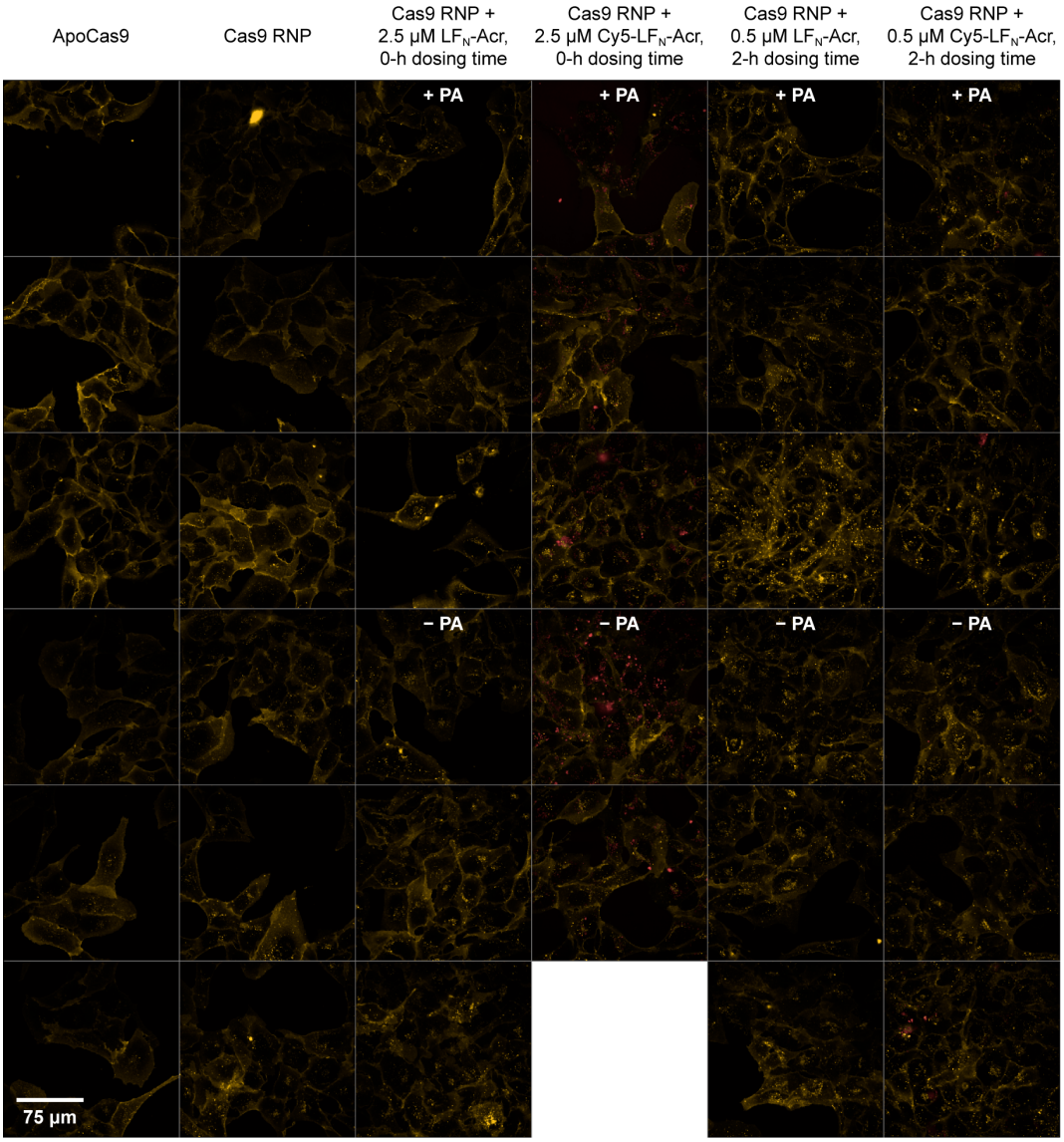


Figure S40C. 568/647 nm channel (continued on the next page).

Downloaded from pubs.acs.org/jacsat/article-supplement/5420577/pdf/ja5c19089_si_001/ by guest on 21 November 2026

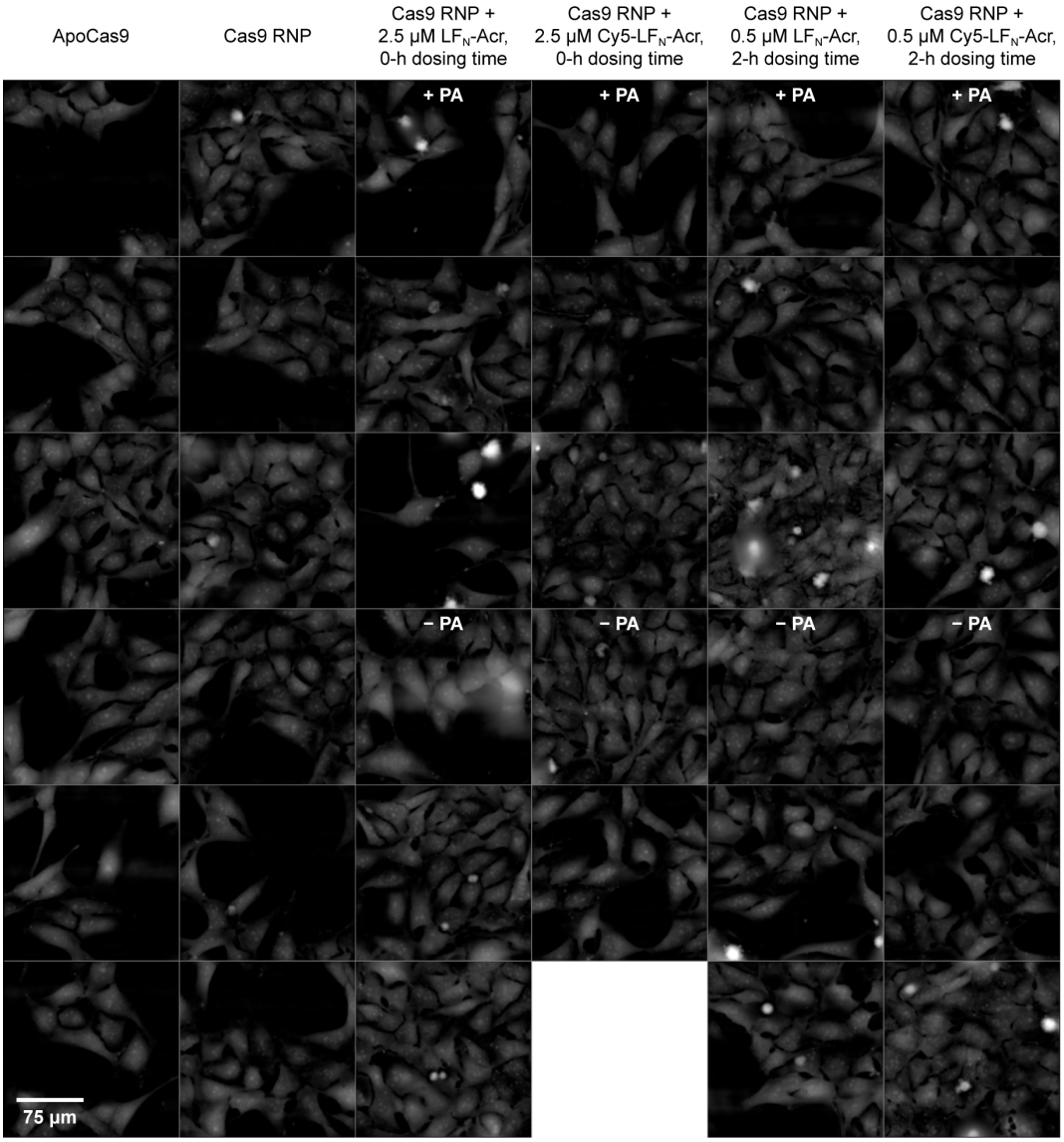


Figure S40D. DPC channel.

Figure S40. Direct visualization of Cy5-LF_N-Acr delivery in the *GFP*-disruption assay. (A–D) SpCas9-NLS RNP (20 pmol) targeting *GFP* was delivered via nucleofection into U2OS-EGFP.PEST cells. The cells were seeded at a density of 20,000 cells per well in 100 μL of culture medium, incubated at 37 °C, and treated with Cy5-LF_N-Acr (0.5–2.5 μM) ± PA (20 nM) at 0 or 2 h. After 30 h, live cells were washed and stained with Hoechst 33342 and WGA555 in FluoroBrite DMEM, then imaged using high-throughput confocal microscopy (60× objective) to detect fluorescence from Hoechst 33342 (blue nuclear marker; 405 nm excitation), WGA555 (yellow cell membrane marker; 568 nm excitation), and Cy5 (red; 647 nm excitation). DPC microscopy was also performed. Controls include nucleofection of Cas9 RNP and nucleofection of Cas9 RNP followed by treatment with LF_N-Acr (0.5–2.5 μM) ± PA (20 nM) at 0 or 2 h. These are the same wells shown in Figure S39, imaged at higher magnification, with the GFP channel omitted. Panels A, B, C, and D contain the 647 nm, 405/647 nm, 568/647 nm, and DPC channels, respectively.

Downloaded from pubs.acs.org/jacsat/article-supplement/5420577/pdf/ja5c19089_si_001/ by guest on 21 November 2026

Plasmid Sequences

pAV13-MBP-TEV-4×NLS-Cys-AcrIIA4-2×NLS

The sequence that encodes 6×His-MBP-TEV-4×NLS-G_4CG_4S-AcrIIA4-GS-2×NLS is in uppercase, and its domains are underlined differently: 6×His-MBP tag, TEV site, 4×SV40 NLS, G_4CG_4S linker, **AcrIIA4**, GS linker, 2×SV40 NLS.

cgtctccgggagctgcatgtgtcagaggttttcaccgtcatcaccgaaacgcgcgaggcagctgcggtaa
agctcatcagcgtggtcgtgaagcgattcacagatgtctgcctgttcatccgcgtccagctcgttgagtt
tctccagaagcgttaatgtctggcttctgataaagcgggccatgttaagggcggttttttcctgtttggt
cactgatgcctccgtgtaagggggatttctgttcatgggggtaatgataccgatgaaacgagagaggatg
ctcacgatacgggttactgatgatgaacatgcccggttactggaacgttgtgagggtaaacaactggcgg
tatggatgcggcgggaccagagaaaaatcactcagggtcaatgccagcgcttcgttaatacagatgtagg
tgttccacagggtagccagcagcatcctgcgatgcagatccggaacataatggtgcagggcgctgacttc
cgcgtttccagactttacgaaacacggaaaccgaagaccattcatgttgttgctcaggtcgcagacgttt
tgcagcagcagtcgcttcacgttcgctcgcgtatcggtgattcattctgctaaccagtaaggcaacccccg
ccagcctagccgggtcctcaacgacaggagcacgatcatgcgcacccgtggccaggacccaacgctgccc
gagatgcgccgcgtgcggctgctggagatggcggacgcgatggatatgttctgccaagggttggtttgcg
cattcacagttctccgcaagaattgattggctccaattcttggagtggtgaatccgttagcgaggtgccg
ccggcttccattcaggtcgaggtggcccggctccatgcaccgcgacgcaacgcggggaggcagacaaggt
atagggcggcgcctacaatccatgccaacccgttccatgtgctcgccgaggcggcataaatcgccgtgac
gatcagcggtccaatgatcgaagttaggctggtaagagccgcgagcgatccttgaagctgtccctgatgg
tcgtcatctacctgcctggacagcatggcctgcaacgcgggcatcccgatgccgccggaagcgagaagaa
tcataatggggaaggccatccagcctcgcgtcgcgaacgccagcaagacgtagcccagcgcgtcggccgc
catgccggcgataatggcctgcttctcgccgaaacgtttggtggcgggaccagtgacgaaggcttgagcg
agggcgtgcaagattccgaataccgcaagcgacaggccgatcatcgtcgcgctccagcgaaagcggtcct
cgccgaaaatgacccagagcgctgccggcacctgtcctacgagttgcatgataaagaagacagtcataag
tgcggcgacgatagtcatgccccgcgcccaccggaaggagctgactgggttgaaggctctcaagggcatc
ggtcgacgctctcccttatgcgactcctgcattaggaagcagcccagtagtaggttgaggccgttgagca
ccgccgccgcaaggaatggtgcatgcaaggagatggcgcccaacagtcccccggccacggggcctgccac
catacccacgccgaaacaagcgctcatgagcccgaagtggcgagcccgatcttccccatcggtgatgtcg
gcgatataggcgccagcaaccgcacctgtggcgccggtgatgccggccacgatgcgtccggcgtagagga
tcgagatctcgatcccgcgaaattaatacgactcactatagggagaccacaacggtttccctctagtgcc
ggctccggagagctctttaattaagcggccgccctgcaggactcgagttctagaaataatttgtttaac
tttaagaaggagatatacatATGAAATCTTCTCACCATCACCATCACCATGGTTCTTCTATGAAAATCGA
AGAAGGTAAACTGGTAATCTGGATTAACGGCGATAAAGGCTATAACGGTCTCGCTGAAGTCGGTAAGAAA
TTCGAGAAAGATACCGGAATTAAAGTCACCGTTGAGCATCCGGATAAACTGGAAGAGAAATTCCCACAGG
TTGCGGCAACTGGCGATGGCCCTGACATTATCTTCTGGGCACACGACCGCTTTGGTGGCTACGCTCAATC
TGGCCTGTTGGCTGAAATCACCCCGGACAAAGCGTTCCAGGACAAGCTGTATCCGTTTACCTGGGATGCC
GTACGTTACAACGGCAAGCTGATTGCTTACCCGATCGCTGTTGAAGCGTTATCGCTGATTTATAACAAAG
ATCTGCTGCCGAACCCGCCAAAAACCTGGGAAGAGATCCCGGCGCTGGATAAAGAACTGAAAGCGAAAGG
TAAGAGCGCGCTGATGTTCAACCTGCAAGAACCGTACTTCACCTGGCCGCTGATTGCTGCTGACGGGGGT

Downloaded from pubs.acs.org/jacsat/article-supplement/5420577/pdf/ja5c19089_si_001/ by guest on 21 November 2026

TATGCGTTCAAGTATGAAAACGGCAAGTACGACATTAAAGACGTGGGCGTGGATAACGCTGGCGCGAAAG
CGGGTCTGACCTTCCTGGTTGACCTGATTAAAAACAAACACATGAATGCAGACACCGATTACTCCATCGC
AGAAGCTGCCTTTAATAAAGGCGAAACAGCGATGACCATCAACGGCCCGTGGGCATGGTCCAACATCGAC
ACCAGCAAAGTGAATTATGGTGTAACGGTACTGCCGACCTTCAAGGGTCAACCATCCAAACCGTTCGTTG
GCGTGCTGAGCGCAGGTATTAACGCCGCCAGTCCGAACAAAGAGCTGGCAAAAGAGTTCCTCGAAAACTA
TCTGCTGACTGATGAAGGTCTGGAAGCGGTTAATAAAGACAAACCGCTGGGTGCCGTAGCGCTGAAGTCT
TACGAGGAAGAGTTGGCGAAAGATCCACGTATTGCCGCCACTATGGAAAACGCCCAGAAAGGTGAAATCA
TGCCGAACATCCCGCAGATGTCCGCTTTCTGGTATGCCGTGCGTACTGCGGTGATCAACGCCGCCAGCGG
TCGTCAGACTGTCGATGAAGCCCTGAAAGACGCGCAGACTAATTCGAGCTCGAACAACAACAACAATAAC
AATAACAACAACCTCGGGATCGAGGAAAACCTGTACTTCCAATCCAATGCCACTCCCAAGAAGAAGCGAA
AGGTGGGTGGGTCCCCAAAGAAGAAACGGAAAGTAGGCGGCTCCCCCAAAAAGAAGCGAAAAGTAGGGGG
TAGCCCCAAGAAGAAGCGGAAGGTAGGTATCCACGGAGTCCCAGCAGCTACCGGCGGTGGTGGTTGTGGT
GGGGGCGGCAGC**ATGAATATTAATGACTTAATTAGAGAAATCAAAAACAAAGATTACACAGTGAAATTGA**
GTGGTACGGATAGCAATAGTATCACACAGCTAATTATTCGCGTTAATAATGATGGCAACGAGTATGTAAT
TTCTGAAAGTGAAAATGAATCAATCGTTGAAAAATTCATCTCTGCATTCAAAAACGGTTGGAATCAAGAA
TACGAGGATGAAGAAGAATTTTATAATGACATGCAAACAATCACCTTAAAAAGTGAGTTGAACGGGTCAC
CTAAGAAAAAACGAAAAGTTGAGGATCCTAAAAAGAAACGAAAAGTTGATACCGGTTAAtaacattggaa
gtggataacggatccgcgatcgcggcgcgccacctggtggccggccggtaccacgcgtgcgcgctgatcc
ggctgctaacaaagcccgaaaggaagctgagttggctgctgccaccgctgagcaataactagcataaccc
cttggggcctctaaacgggtcttgaggggtttttgctgaaaggaggaactatatccggatatccacagg
acgggtgtggtcgccatgatcgcgtagtcgatagtggctccaagtagcgaagcgagcaggactgggcggc
ggccaaagcggtcggacagtgctccgagaacgggtgcgcatagaaattgcatcaacgcatatagcgctag
cagcacgccatagtgactggcgatgctgtcggaatggacgatatcccgcaagaggcccggcagtaccggc
ataaccaagcctatgcctacagcatccagggtgacggtgccgaggatgacgatgagcgcattgttagatt
tcatacacggtgcctgactgcgttagcaatttaactgtgataaactaccgcattaaagcttatcgatgat
aagctgtcaaacatgagaattcttgaagacgaaagggcctcgtgatacgcctatttttataggttaatgt
catgataataatggtttcttagacgtcaggtggcactttcggggaaatgtgcgcggaacccctatttgt
ttatttttctaaatacattcaaatatgtatccgctcatgagacaataaccctgataaatgcttcaataac
attgaaaaaggaagagtatgagtattcaacatttccgtgtcgcccttattccctttttgcggcattttg
ccttcctgtttttgctcacccagaaacgctggtgaaagtaaaagatgctgaagatcagttgggtgcacga
gtgggttacatcgaactggatctcaacagcggtaagatccttgagagttttcgccccgaagaacgttttc
caatgatgagcacttttaaagttctgctatgtggcgcggtattatcccgtgttgacgccgggcaagagca
actcggtcgccgcatacactattctcagaatgacttggttgagtactcaccagtcacagaaaagcatctt
acggatggcatgacagtaagagaattatgcagtgctgccataaccatgagtgataacactgcggccaact
tacttctgacaacgatcggaggaccgaaggagctaaccgcttttttgcacaacatgggggatcatgtaac
tcgccttgatcgttgggaaccggagctgaatgaagccataccaaacgacgagcgtgacaccacgatgcct
gcagcaatggcaacaacgttgcgcaaactattaactggcgaactacttactctagcttcccggcaacaat
taatagactggatggaggcggataaagttgcaggaccacttctgcgctcggcccttccggctggctggtt
tattgctgataaatctggagccggtgagcgtgggtctcgcggtatcattgcagcactggggccagatggt
aagccctcccgtatcgtagttatctacacgacggggagtcaggcaactatggatgaacgaaatagacaga
tcgctgagataggtgcctcactgattaagcattggtaactgtcagaccaagtttactcatatatacttta

Downloaded from pubs.acs.org/jacsat/article-supplement/5420577/pdf/ja5c19089_si_001/ by guest on 21 November 2026

gattgatttaaaacttcatttttaatttaaaaggatctaggtgaagatccttttttgataatctcatgacc
aaaatcccttaacgtgagttttcgttccactgagcgtcagaccccgtagaaaagatcaaaggatcttctt
gagatccttttttttctgcgcgtaatctgctgcttgcaaacaaaaaaaccaccgctaccagcggtggtttg
tttgccggatcaagagctaccaactctttttccgaaggtaactggcttcagcagagcgcagataccaaat
actgtccttctagtgtagccgtagttaggccaccacttcaagaactctgtagcaccgcctacatacctcg
ctctgctaatcctgttaccagtggctgctgccagtggcgataagtcgtgtcttaccgggttggactcaag
acgatagttaccggataaggcgcagcggtcgggctgaacgggggttcgtgcacacagcccagcttggag
cgaacgacctacaccgaactgagatacctacagcgtgagctatgagaaagcgccacgcttcccgaaggga
gaaaggcggacaggtatccggtaagcggcagggtcggaacaggagagcgcacgagggagcttccagggggg
aaacgcctggtatctttatagtcctgtcgggtttcgccacctctgacttgagcgtcgatttttgtgatgc
tcgtcaggggggcggagcctatggaaaaacgccagcaacgcggccttttacggttcctggccttttgct
ggccttttgctcacatgttctttcctgcgttatcccctgattctgtggataaccgtattaccgcctttga
gtgagctgataccgctcgccgcagccgaacgaccgagcgcagcgagtcagtgagcgaggaagcggaagag
cgcctgatgcggtattttctccttacgcatctgtgcggtatttcacaccgcaatggtgcactctcagtac
aatctgctctgatgccgcatagttaagccagtatacactccgctatcgctacgtgactgggtcatggctg
cgccccgacacccgccaacacccgctgacgcgccctgacgggcttgtctgctcccggcatccgcttacag
acaagctgtgac

Downloaded from pubs.acs.org/jacsat/article-supplement/5420577/pdf/ja5c19089_si_001/ by guest on 21 November 2026

Equations

$$\text{Normalized Cas9 specificity without Acr} = \frac{\text{On/OT Cas9}}{\text{On/OT Cas9}} = 1 \tag{S1}$$

$$\text{Normalized Cas9 specificity with Acr} = \frac{\text{On/OT Acr–inhibited Cas9}}{\text{On/OT Cas9}} = 1.10 - 1.41 \tag{S2}$$

$$\text{Increase in Cas9 specificity with Acr} = \frac{\text{Normalized Cas9 specificity with Acr} - \text{Normalized Cas9 specificity without Acr}}{\text{Normalized Cas9 specificity without Acr}} \times 100\% = 10 - 41\% \tag{S3}$$

$$\text{Total increase in Cas9 specificity with Acr} = \text{Increase in Cas9 specificity with Acr (On/OT1)} + \text{Increase in Cas9 specificity with Acr (On/OT2)} + \text{Increase in Cas9 specificity with Acr (On/OT3)} + \text{Increase in Cas9 specificity with Acr (On/OT4)} = 90\% \tag{S4}$$

Downloaded from pubs.acs.org/jacsat/article-supplement/5420577/pdf/ja5c19089_si_001/ by guest on 21 November 2026

References

(1) Staahl, B. T.; Benekareddy, M.; Coulon-Bainier, C.; Banfal, A. A.; Floor, S. N.; Sabo, J. K.; Urnes, C.; Munares, G. A.; Ghosh, A.; Doudna, J. A. Efficient genome editing in the mouse brain by local delivery of engineered Cas9 ribonucleoprotein complexes. *Nat. Biotechnol.* **2017**, *35*, 431–434.

(2) Vera, A. O.; Truex, N. L.; Sreekanth, V.; Pentelute, B. L.; Choudhary, A.; Raines, R. T. Protective antigen–mediated delivery of an anti-CRISPR protein for precision genome editing. *Proc. Natl. Acad. Sci. U. S. A.* **2025**, *122*, e2426960122.

(3) Kapust, R. B.; Tözsér, J.; Fox, J. D.; Anderson, D. E.; Cherry, S.; Copeland, T. D.; Waugh, D. S. Tobacco etch virus protease: Mechanism of autolysis and rational design of stable mutants with wild-type catalytic proficiency. *Protein Eng.* **2001**, *14*, 993–1000.

(4) Cong, L.; Ran, F. A.; Cox, D.; Lin, S.; Barretto, R.; Habib, N.; Hsu, P. D.; Wu, X.; Jiang, W.; Marraffini, L. A. Multiplex genome engineering using CRISPR/Cas systems. *Science* **2013**, *339*, 819–823.

(5) Sreekanth, V.; Zhou, Q.; Kokkonda, P.; Bermudez-Cabrera, H. C.; Lim, D.; Law, B. K.; Holmes, B. R.; Chaudhary, S. K.; Pergu, R.; Leger, B. S.; Walker, J. A.; Gifford, D. K.; Sherwood, R. I.; Choudhary, A. Chemogenetic system demonstrates that Cas9 longevity impacts genome editing outcomes. *ACS Cent. Sci.* **2020**, *6*, 2228–2237.

(6) Reyon, D.; Tsai, S. Q.; Khayter, C.; Foden, J. A.; Sander, J. D.; Joung, J. K. FLASH assembly of TALENs for high-throughput genome editing. *Nat. Biotechnol.* **2012**, *30*, 460–465.

(7) Cowan, C. A.; Klimanskaya, I.; McMahon, J.; Atienza, J.; Witmyer, J.; Zucker, J. P.; Wang, S.; Morton, C. C.; McMahon, A. P.; Powers, D.; Melton, D. A. Derivation of embryonic stem-cell lines from human blastocysts. *N. Engl. J. Med.* **2004**, *350*, 1353–1356.

(8) Liu, Y.; Zou, R. S.; He, S.; Nihongaki, Y.; Li, X.; Razavi, S.; Wu, B.; Ha, T. Very fast CRISPR on demand. *Science* **2020**, *368*, 1265–1269.

(9) Pomerantsev, A. P.; McCall, R. M.; Chahoud, M.; Hepler, N. K.; Fattah, R.; Leppla, S. H. Genome engineering in *Bacillus anthracis* using tyrosine site-specific recombinases. *PLoS Biol.* **2017**, *12*, e0183346.

(10) Singh, Y.; Chaudhary, V. K.; Leppla, S. H. A deleted variant of *Bacillus anthracis* protective antigen is non-toxic and blocks anthrax toxin action in vivo. *J. Biol. Chem.* **1989**, *264*, 19103–19107.

Downloaded from pubs.acs.org/jacsat/article-supplement/5420577/pdf/ja5c19089_si_001/ by guest on 21 November 2026